CHAPTER 6

MINE EXPLOSION ANALYSIS

By
A. Green

Following a mine explosion there is a need to establish the factors that led to the incident in order that the incident can be made avoidable in future. This objective can only be achieved by thorough investigation and analysis of the incident. Collection of data and its analysis is not straight forward because:

- The source of ignition can be well away from the centre of maximum heat damage or maximum pressure damage.
- The positions of objects found following the explosion are not necessarily the positions of those objects prior to the explosion.
- Maximum heat damage does not necessarily occur with maximum pressure damage.
- The time elapsed.
- Delayed access to the site.

As a consequence, detailed calculations are required to establish the pressures and movement of objects that were likely to exist during the explosion and from which different hypotheses on the course and cause of the explosion can be tested.

This chapter contains a brief outline of research methods and a detailed discussion on the movement of objects and modelling techniques which assist the investigation process.

Finally these techniques are applied to the explosion at Moura No.4 Mine, based on the data taken by persons at the time of the investigation and given as evidence to the Inquiry.

6.1 Investigation Techniques

In any investigation with an explosion (whether mine or otherwise) it is essential to obtain as much data as possible so that the incident can be reconstructed. For example, following an overseas hotel bombing, several thousand buckets of blast fragments were collected from this hotel and surrounding area to assist with the reconstruction in the explosion. In the case of the Lockerbie plant disaster, plane fragments were collected and reassembled to establish the location and size of the bomb on the aircraft. Although this approach is mainly applied to bombs, the same philosophy can be applied to mine explosions. In the Golborne mine explosions, [24] detailed examination of the ventilation system followed by modelling of the ventilation established the course of the build up of methane in the mine which subsequently was ignited.

In all these cases, the first objective was to establish the course of the explosion. This is achieved by systematically looking at pressure, heat, flow and other directional indicators.

The way the pressure develops relative to the way maximum heat damage occurs, or indicators of the direction of flow can be used to establish a set of criteria against which different hypotheses can be tested.

Often there are one or two factors that are decisive in establishing the area of ignition. In the Flixborough explosion [25] for example, directional indications from lamp posts on the site blown over by the air movement caused by the explosion indicated the area from which the explosion developed. Further investigation of pipework in that area established which pipe in the area had fractured and what had occurred.

Once the course of the explosion has been established, then factors leading to the cause of the explosion can be identified. Usually more than one factor is responsible for the explosion.

To complete the analysis, alternative hypotheses have to be tested against the critical factors on the course of the explosion and then against the requirements for a build-up of a flammable mixture, and an ignition source. Explosions resulting from large gas leaks in surface installations can be triggered by any one of numerous sources. Underground, ignition sources are well controlled and so there is a need to establish both the mechanism of obtaining the flammable mixture and the mechanism for ignition. The normal procedure is to concentrate on well known sources in the area and excluding them before looking at more exotic sources. Often there is more than one mechanism both for flammable mixture build up and for ignition. This highlights the need to establish a course for the explosion as it limits the number of potential ignition sources. Generally the larger the area considered, the more ignition sources there are in that area. For example, the Moura explosion has ten potential mechanisms for ignition between 23 c/t and the goaf in the Main Dips area of the mine. The Inquiry only considered 3 in detail, namely frictional ignition from rock and from the Entonox bottle, and the flame safety lamp.

6.2 Australian and Overseas Forensic Research

Research into explosion debris analysis has centred on three main areas:

- Eestimating overpressures by the type and amount of damage incurred.
- Estimating overpressures from the movement of objects.
- Estimating flame pattern from the heat damage incurred to objects.

Physical models of the incident are used to study flame development and propagation allowing the researchers to piece together the relative timing of different events and to show how the observed patterns of pressure, heat and air flow have been obtained by Hjertager [26] and more recently mathematical models are being used for this purpose as well Hjertager [27].

Pressure and heat effects on materials are time dependent. The mechanical damage is related to the impulse (that is the pressure-time integral) received from the explosion at the material surface. Heat damage is related to the heat impulse (that is the heat flux-time integral) at the material surface. Obviously a large pressure pulse over a short duration will give the same degree of damage as a pulse 1/10th as high over 10 times the previous duration as long as the threshold to damage is exceeded. This is similar with the degree of heat damage. Studies of typical damage due to pressure or heat where the time duration is known, gives a baseline against which actual incidents can be compared. It is this process that provides the basis for analysis of the course of an explosion.

6.2.1 Estimating Overpressures from Damage to Structures

Table 6.1 contains the range of overpressures observed for different degrees of observed damage to buildings and other structures. The table is compiled from various sources and is based on data from chemical and nuclear explosions. In general the overpressures are typical of the onset of such damage. They are valuable in defining the minimum overpressures for such damage.

The data on the collapse of a brick wall can be applied directly to the collapse of brick stoppings in a mine explosion. From Table 6.1 various levels of brick damage occur depending on which source reference, the type of bonding and the type of reinforcing in the wall. Collapse of unreinforced 16″ blocks of the type used at Moura occurs at about 30 kPa.

Christopherson [28] has shown that the response of a brick panel to an unsteady lateral pressure can be described by a simple equation involving the average deflection of the wall, the mass of the wall, the pressure as a function of time and a function describing the resistance of the wall with time. Knowledge of the pressure function and resistance function allows computation of the deflection time history and the time at which the wall collapses. Wiehle and Bockholt [29], Wiehle and Bockholt [30], Wiehle [31] calculated the resistance functions for a given maximum deflection corresponding to the maximum deflection for the elastic phase. After cracking the resistance per unit width decreases linearly to zero at a deflection equivalent to the wall themselves. Such an analysis allows the initial debris velocity and damage to be calculated.

Cantilevered structures such as the long exposed ends of roof bolts, barrier supports etc can also be used to assess the overpressure. A transient pressure pulse can cause rotation of the structure about a point near to its fixing point, if the resistance to movement is overcome by the pressure force. The final deflection can be related to the movement by pressure force and the inertia about the plastic hinge that is formed Roberts and Pritchard [32].

6.2.2 Displacement of Objects

The movement of objects by the explosion is governed by the basic equation of motion where the acceleration is related to the incident pressure through an acceleration coefficient and the resistance to movement. Integration of the equation will yield the velocity and displacement of the object. This method can be used to calculate the distance any object has been displaced, whether a mine rover, bricks, pieces of steel or people. Fletcher and Bowen [33], Longinow [34] and Fletcher et al [35].

Objects and people can be in a number of orientations relative to the incident blast wave, upright or prone, side on or face on etc. For many objects the centre of mass is not at the same height as the centre of drag. Consequently orientation of the object will change during the motion. Any calculations based on maximum exposed area will lead to the minimum explosion pressure required to move the objects a given distance.

Various studies Bowen et al [36], Iverson [37] and Fletcher et al [38] and Harris [39] have been done on the fragmentation and displacement of windows in surface explosions. However, few studies have been done on materials directly applicable to the movement of objects in mine explosions.

A number of experiments have been undertaken to look at the behaviour of bodies as they are displaced by the blast. Taborilli et al [40] examined the velocity and distance histories of anthropomorphic dummies. The most interesting observation as shown in Figure 6.1, is the way the head and feet move relative to the centre of mass. Michelis [41] repeated this type of experiment at Tremonia explosion gallery with dummies wearing miner's helmets, cap lamp, belt, battery and self rescuer. He found that the head was displaced forward. The difference in the result is due to the centre of mass being lowered while the centre of drag is raised compared with the former study.

The work on deceleration of mannequins suggests that body alignment is not retained for more than a few metres. The bodies at Moura were not in random orientations and as will be shown in Section 6.2.3 have moved a considerable distance. There seems to be a disagreement between what was observed at Moura and overseas work on body alignment. It should be noted, however, that the work done overseas was (1) on hard surfaces (concrete) unlike the compacted floor of a mine roadway and (2) the bodies were subjected to no impulse or one that had a static pressure impulse of similar duration to the dynamic impulse. These two conditions are very different from a mine explosion and could be the reasons for the discrepancy. There is however a need for much more detailed research in this area for mine explosions.

6.2.3 Heat Damage

Heat damage to plastic materials, fibres and other surfaces is highly

dependent on the incident heat flux and the duration of flame. Brookes and Rae [42] showed that a radiant coal dust explosion will produce varying degrees of blistering in a single entry heading, with no samples showing signs that they had reached their ignition temperatures and only a few showing evidence of pyrolysis.

The recent development of better test methods of assessing the fire behaviour of materials Brabauskas [43], Green et al [44] and Green et al [45] give the correlation between flame residence time and time to ignition for a given material. That correlation can be used to assess flame residence times in explosions from microscopic examination of materials in the incident.

There has been very little work on the effect of long residence times under explosion conditions, i.e. high incident heat fluxes, due to the restriction in geometry of experimental galleries around the world.

6.3 Modelling of Explosions

There are two broad classes of modelling techniques that can be used to assist in understanding how an explosion will develop in complex and confined geometrics: Physical and Mathematical models. The former generate physical data which can be compared with the explosion case to be studied. Mathematical models generate details of the physics that cannot be measured in practice and can give both a qualitative and quantitative understanding as to what has occurred.

6.3.1 Physical Models

Physical models are full or scaled models of the case to be studied. Since explosions are very complex phenomena, there is a limit as to how small a model can be made and still yield results of use. Since explosions are fluid problems, similarity in the fluid flow should be maintained if at all possible. For example, the Reynolds number is one parameter that characterises air flow in a mine roadway. Any model of the roadway should have a similar Reynolds number in addition to being geometrically scaled. In practice, this requires the velocity or viscosity to be changed as the dimensions are changed.

Full and scaled models are being used to assist investigation of accidents. After the Kings Cross Fire in London, UK, a 1/3rd and 1/50th scale model of the conveyor system were constructed by the HSE and Edinburgh University to assist with the investigation. Currently the Christian Michaelson Institute is building a scale model of the piper Alpha Oil Platform to assist the Norwegian Government with continued investigation of that accident.

In an explosion there are about 20 dimensionless parameters similar to the Reynolds number which control different processes. It is impossible to scale more than one of these accurately so models at a reduced scale can only be used as a qualitative guide of what is occurring.

A 1:54 scale model of a section of the Moura No.4 Main Dips Section was constructed between 25 c/t and 27 c/t over all roadways to help visualise the changes that occur when the ignition source is systematically moved around the model under controlled conditions.

6.3.2 Mathematical Models

Over the last few years mathematical modelling of fires has been used to assist with the investigation of serious fires. Most of this work has been pioneered by Dr G. Cox at the Fire Research Establishment, Barhamwood, UK [46]. Among the application of these field techniques were the Bradford Football Stadium Fire and the Kings Cross fire. The UKAEA establishment at Harwell also undertook studies on the Kings Cross fire which pointed the way for experimenters to confirm what actually occurred.

The use of modelling techniques for explosion accidents is somewhat more limited. Currently there is some work being undertaken by Hjertager on the Piper Alpha explosion but this is in a very early stage of development. The only other work in this area is being undertaken by Green who is applying his own code to the problem in hand concerning Moura No.4 Mine.

An explosion involves a propagating pressure front with gases at high temperature and pressure following it. The temperatures may be high enough to ignite gas and may contain a flame front as well. Hence an explosion simulation has to include prediction of the fluid flow and combustion. The fluid flow itself is a complex phenomenon with the effects of convection and diffusion brought about by viscosity and turbulence. Combustion adds to this complication and requires chemical kinetics to handle it.

Any general flow is governed by the Navier Stokes equations and these are used in conservative form with additional equations for gas species written in terms of fuel mass fraction and mixture fraction. A two equation model of turbulence, the K - Epsilon model, is used to describe the effects of turbulence. A simple one step combustion process is used because a reaction scheme for methane involves 54 basic reactions. Solving these equations can be done but is computationally very expensive. A simplified approach is justified given the complexities in solving the flow equations.

Eight equations have to be solved simultaneously for a 2 dimensional flow (9 for a 3D case). Only a few methods have been used to solve combustion problems of this type. One method employed by Hjertager [47] is based on the SIMPLE method by Pantanka and Spalding [48]. This is an implicit method which in principle can use any value of timestep. This claim is justified when it comes to steady state problems, but with transient flows there is always a timestep limitation. Another method is the Flux Corrected Transport (FCT) method of Boris and Oran [49]. This is an explicit method and so has

a limitation on the timestep value for steady state and transient problems. The advantage of the FCT method is that it can control numerical diffusion in the solution so that shock fronts remain as shock fronts and do not degrade.

The method that is being developed by Green and Srinivas [50] to solve the equation set is a Total Variation Diminishing (TVD) scheme and is similar to the FCT method, being able to control numerical diffusion in the solution. The region to be simulated is divided into finite volumes and for each of the volumes a modified Runge-Kutta method is used to solve the governing equations. This scheme has some very desirable properties:

- The scheme is explicit and consequently boundary conditions are easily implemented.
- A larger timestep can be used compared with other explicit codes.
- The scheme renders itself to parallel processing. This feature can make an explicit scheme yield a solution far more quickly than an implicit scheme even though the latter can accept a higher timestep size.
- The code can readily be setup with body fitted coordinates so that explosions in very complex geometrics can be studied.
- Additional diffusion is used to handle large pressure gradients through an artificial diffusion term. This acts as a diffusion limiter and compensates for the numerical diffusion in the solution.

In running the code the procedure given below is used. The code has been written for a parallel architecture, such as found on a transputer system, where the code is partitioned according to the geometry of the problem to be solved and the number of processors available. The same size problem should therefore take (much) less time to run than on a single processor.

The procedure for the calculation is the same for both scalar and parallel schemes:

- The geometry of the problem is divided onto a grid defining finite volumes or cells and when run in a parallel configuration cells are automatically grouped together to share the computational work equally between processors and with minimum communication between processors.
- The starting conditions for each cell are provided.
- A timestep is calculated for each cell based on Courant number considerations. The global minimum is used throughout the next timestep calculation.

. Artificial Dissipation and viscous flux terms are calculated for each cell and are then kept frozen through the four levels of the solving algorithm at each timestep.

. The convective fluxes are summed for every cell and at every sweep of the solving algorithm.

. Boundary and source terms are calculated.

. The new solution is calculated and steps 5 and 6 are repeated for the four levels of the solver.

. Steps 3 to 7 are repeated until the desired level of real time is reached. Data values are periodically written to disc according to user requirements.

The code has been validated against a number of aerodynamic and combustion problems. Figure 6.2 shows the pressure measured experimentally for a 10m ignition tube with rings at two locations. Figure 6.3 shows the computed solution for the same locations. As can be seen good agreement both on the overall shape and magnitude is obtained. Further work to validate the code against velocity and turbulent data for an explosion is in hand. This process will take several months. In the meantime this work is being used in an uncalibrated state on the Moura Explosion to gain insight into the processes which are occurring during the explosion and the likely sequence of events.

6.4 Reanalysis of the Moura No.4 Mine Explosion

At the Inquiry, the only evidence pertaining to the establishment of the course of the explosion was that given by Green [51]. Pressure and air velocities were presented based on the destruction of brick stoppings. In that analysis the velocities and distances were calculated using a specific case for the equations of motion which did not include the deceleration phase of the brick on impact with the ground. In the re-analysis that follows a more general equation of motion is used which did not include the deceleration phase.

In the original evidence, calculation involving the movement of the shuttle cars, the mine rover and the continuous miner were all based on assumptions of the direction of the blast. With the presentation of an alternative hypothesis by Leivesley and Romaniuk [2], this original assumption was called into question. A reanalysis of the movement of miscellaneous objects is presented based on the more general equation of motion with associated deceleration phase.

The velocities pressures and impulses obtained in the reanalysis were then applied to the likely movement of bodies, to define the likely distances such objects would have been moved.

6.4.1 Brick Stoppings

The analysis of the distribution of debris follows that by Fletcher et al [35]. In this analysis the displacement X is given by:

$$\frac{d^2X}{dt^2} = a\,P - F$$

where t is the time, a is the acceleration coefficient which is a function of the drag coefficient, the mass of the object and cross-sectional area presented to the oncoming blast wave. P is a pressure function which mimics the force applied to the object. F is a friction function.

For brick stoppings, the pressure function is assumed to be dependent on the dynamic pressure as the equilibration of the static pressure over 0.08m is 3ms, much shorter than the timescale for the dynamic pressure (150-800ms). The friction factor F is assumed to be a simple function of the weight of the brick. The coefficient of friction is taken as 0.1. This is less than the value normally assumed for an object moving over a surface (0.3) to account for:

- The effect of powdered compacted coal dust and limestone dust on the floor (a reduction of approximately 33%); and
- The effect of some bouncing rather than strict translational movement along the floor (a reduction of 50%).

Such a low value for the friction coefficient leads to a minimum range of velocity and pressure.

Table 6.2 contains the maximum and minimum distances that a brick will move for a given velocity. The maximum distance is based on a brick 2.5m above the ground, while the minimum distance gives that of a brick 0.25m above the ground. Four cases are considered, each with a different duration for the wind blast; 100ms, 200ms, 400ms, 600ms respectively. The impulse on the brick has been calculated and is also given in Table 6.2. Figure 6.4 shows the maximum and minimum distances that a brick from a stopping will move for a given impulse. The curves given in this figure are not dependent on the wind duration. Consequently the calculated impulse from brick stoppings can be used to relate the loadings on objects whose position before the explosion were not known.

The damage to brick stoppings submitted to the inquiry is contained in Table 6.3. The velocity range based on the four different wind durations is given in Table 6.4 The damage to the stoppings are best correlated with the associated impulse, (that is the pressure time integral) on the bricks. The associated range of impulses are also given in the table. In the original report by Green [51], the estimation of static pressure was based on the acoustic approximation of Rae. There has been some criticism that the estimated pressures were too high. This criticism seems to have ignored the size of the

estimated errors stated in that report. In this report an alternative and more accurate method has been employed. The pressures are computed from shock wave considerations and are included in Table 6.4.

The reanalysis has given values for the velocities that are consistent with those obtained from those presented at the Inquiry, and which show the same trend. The computed pressures are lower than those given to the inquiry but follow the same trend and are towards lower limit values stated at the Inquiry. The exact values are dependent on the duration of the winds. The wind duration is no longer than 0.6 seconds as a longer time would fail to knock down the stoppings in 27 c/t and 21 c/t (north side). As will be shown later modelling techniques can be used to decrease the uncertainty in this value. The range of impulses however is not as dependent on this factor and can be used to estimate the travel of other objects.

The main feature of this reanalysis is confirmation of the development of pressure away from 27 c/t in a uniform and consistent manner similar to that presented at the original inquiry.

6.4.2 Movement of the Shuttle Cars

In the original analysis, it was tacitly assumed that the direction of blast would be along No.3 Belt Road rather than down 26 c/t. This assumption is questionable in the light of [2]. In this reanalysis Shuttle Car No.30 is assumed to rotate about the end near to the continuous miner due to a targeted force created by a wind blast coming down 26 c/t from No.4 Supply Road.

The equation of motion is similar to that used in the preceding section. The equation relates angle of rotation about a vertical axis, ϕ, to the moments of applied force and resistance

$$\frac{d^2\phi}{dt^2} = a P - a_1 f$$

a is an acceleration coefficient dependent on the drag coefficient, the area over which the pressure force is applied, the distance of the applied force from the point of pivoting, and the moment of inertia. P is the applied pressure which, for the same reason as the brick stopping calculation, is taken as the dynamic pressure. a_1 is a deceleration coefficient dependent on the distance to the centre of mass and the moment of inertia.

The friction factor F is assumed to be a function of the shuttle car mass (18 tonnes). The coefficient of friction will be close to 1.0 until the shuttle car starts to move after which it will be expected to drop towards a value of 0.3, typically found for one surface moving over another.

Integration of this equation with a friction coefficient of 1.0 will thus

yield the minimum angle through which the shuttle car will move. The distance that the end of the shuttle car moves sideways rotating about the other end is given in Table 6.5 for the four wind durations considered in Section 6.2.1. This distance as a function of the applied impulse is given in Figure 6.5. The brick stoppings at 26 c/t, 25 c/t on the north wide and 25 c/t on the south side had impulses in the range 4.2kPa.s and 6.6kPa.s. A linear interpretation on these three points would put the impulse at 26 c/t and No.3 Belt Road, between 4.6kPa.s and 5.6kPa.s.

These values are shown on Figure 6.5 and correspond to movement of s/c No.31 of between 0.6m and 0.9m. It should be emphasised that this range is a minimum. A coefficient of friction of 0.3 would yield a range of movement of between 2.0m and 3.5m.

This analysis confirms that the s/c No.31 has been moved sideways with an impulse consistent with that on the brick stoppings adjacent to this area of the mine. The direction of the wind blast would have to have been along 26 c/t from No.4 Supply Road to cause observed position of the shuttle car against the south rib. A wind blast along 26 c/t from the south goaf would have moved the shuttle car towards the north rib. This is not observed. Furthermore, not only would a wind force along No.3 Belt Road from the goaf not have moved s/c No.31, s/c No.30 would have been blown against the outbye rib rather than finishing toward the inbye rib. The wheel angle on this latter vehicle would suggest some movement, which could be achieved by a wind along No.3 Belt Road from the boot end of the conveyor. However a force from this direction would not move s/c No.31. The slight movement of s/c No.30 could be caused by a vortex shedding around s/c No.31. This would have been a clockwise rotation looking from above and is in the correct direction to achieve the observed movement.

6.4.3 Movement of the Bodies

At the Inquiry no consideration was given as to the position of bodies before the explosion. A brief analysis of the likely distances that the bodies were moved is given. The analysis is the same as that given in section 6.2.1. The friction factor, f, is taken as that given by Fletcher and Bowen [33] for a body undergoing decelerative tumbling. Two body positions are considered; Standing face (or back) to the wind and standing side on to the wind. The acceleration coefficients for these two postures were taken from Table 2.2.1 of Hadjipavlou and Carr-Hill [52].

The body displacement for the four wind durations considered previously are given in Table 6.6. The distance travelled is plotted as a function of Impulse in Figure 6.6. The three bodies found near 26 c/t and No.4 Supply Road would have been subjected to an impulse of between 4.3kPa.s and 5.2kPa.s. This corresponds to a displacement of between 5m and 26m. The impulse in the region of 26 c/t and No.3 Belt Road as indicated in Section 6.2.2 is between 4.6kPa.s and

5.6kPa.s. This corresponds to a displacement between 8m and 29m.

This analysis confirms:

. That the bodies would have been moved by the explosion some considerable distance.

. That the three bodies in the vicinity of the crib room would have been moved less than the others.

6.4.4 Discussion

In this analysis an alternative method, to that presented at the Inquiry, was used to calculate the pressures, impulses and air velocities required for the observed damage. The reanalysis confirms the trends in pressures away from the goaf in the earlier analysis. The calculated pressures in this reanalysis are lower than the mean pressures calculated previously but are within the error estimated in the previous report. Modelling studies are required to elucidate the likely time duration of the winds in this explosion and hence the likely pressures involved.

There are two additional points of interest. Preliminary calculation for the movement of other items in the area around the crib room and No.4 Supply Road suggest that similar impulses to that at the brick stopping have moved objects around the mine. This analysis has not been completed due to the deadlines in preparing this report. There is, however, one exception. The MPV tray in 25 c/t that moved from the stopping across No.4 Supply Road could not have moved this distance without a much larger impulse on this object. This seems to be an anomaly but could be explained by an accelerating flow along No.4 Supply Road. This hypothesis involves interaction of the reflected pressure wave from the rib in No.5 North Return Road after breaking the stopping, with the combustion wave moving out along No.4 Supply Road.

Initial calculation would suggest that only the stoppings at 26 c/t and 25 c/t would have produced this type of interaction as further outbye, the reflected wave would arrive too early to interact with the combustion wave. This process would account for distribution of material from the crib room and the apparently strong wind velocity moving along 26 c/t towards No.3 Belt Road. This hypothesis is only tentative at this stage and could only be shown to be correct from modelling the system.

The second point relates to the water barrier in No.3 Belt Road between 24 c/t and 23 c/t. The calculated impulses on these barriers from the earlier report are between 1.5kPa.s and 1.7kPa.s.

Although these values could be in error due to the dominant effect of the mass of water in the tubs at the time of the explosion (an unknown factor), they are much lower than the values of the

stoppings on either side. This would suggest that the barriers were having a positive effect in quenching the explosion even though the explosion was eventually quenched by water in the swilly. However, their position in the absence of the swilly would not have quenched this explosion. It is therefore recommended that further work on barrier location for this type of mining system be undertaken, involving modelling studies.

This reanalysis shows positively that the shuttles were moved by the explosion to their observed position. Only a flow along 26 c/t from No.4 Supply Road towards No.3 Belt Road could have produced this result. This should be taken as a very positive indication in discussions on the course of the explosion (see Chapter 7).

The reanalysis also shows that the bodies of the miners killed would have been moved some considerable distance with those nearer to No.3 Belt Road being moved on average further than those near to No.4 Supply Road. There is a question mark that needs further research, over whether or not the alignment of bodies observed at Moura were coincident or not. A preliminary statistical analysis would suggest not but this seems at odds with research in the UK and the USA. It is not clear from the work of Michelis whether the alignment that he found is totally random or whether it is within a narrow sector confined to $\pm 45°$ from the axis of flow.

6.5 Modelling Studies

6.5.1 1:54 Scale Model Experiments

A 1:54 scale model of part of the Main dips section of Moura No.4 Mine was constructed in a manner that it could be easily extended to cover a larger area of the mine. The model was of the area between 25 c/t and 27 c/t across all headings and included part of the goaf. This area is shown in Figure 6.7 together with the positions of 4 pressure and 6 flame sensors. Each experiment was also monitored with high speed cameras and video cameras.

A number of experiments have been carried out in which the ignition point has been systematically varied with the objectives:

. Identify the differences in flows from different ignition sources.

. Measure the relative time of arrival and direction of blast at the positions of the mine rover and shuttle cars.

. Measure the relative flame duration at the mine rover and at the shuttle cars.

The ignition points were chosen as representative alternative ignition locations to test how moving the ignition would affect the interpretation of the evidence given at the Inquiry and involved in the preceding section. The ignition points are also given in Figure 6.8.

For example ignition at point 1 is intended to simulate an ignition in the crib room. In some scenarios ignition has started in the goaf. Since most of the goaf is not included in the model, simulation near 27 c/t (north side) for example, is simulated by ignition at point 2, whereas ignition deeper in the goaf (north side) is simulated by simultaneous ignition at points 2 and 3, in an attempt to take some account of the increased strength and wider dispersion of such an ignition before it enters the area depicted by the model.

In each experiment, a methane air mixture was circulated throughout the model prior to ignition with matchhead detonators. The gas concentration was monitored until a steady concentration was observed throughout the model.

One of the problems encountered was that of achieving a uniform concentration throughout the model. A number of alternative recirculation patterns and techniques were tried before obtaining a satisfactory distribution throughout the model ($\pm$ 0.5%).

A uniform gas distribution was used throughout in an attempt to simulate total fuel conditions prevailing at the time of the incident. In any scenario of ignition, a goaf roof fall must have occurred to obtain enough fuel in the atmosphere to propagate an explosion. This fuel could have been either methane, coal dust or a combination of the two. The total fuel content would have been evenly distributed throughout the area of the mine by the wind blast accompanying the fall of the goaf. Furthermore, coal dust would also have been picked up by the explosion. Given other limitations of the model such as size, a uniform gas distribution is a reasonable starting point for simulation of a total gas and coal dust mixture.

In the time available to the project only a limited number of experiments have been undertaken. In all experiments, the brick stoppings were simulated by balsa wood partitions, but no models were used to represent the positions of the miner, mine rover, shuttle cars or conveyor belt. Although at the outset this was intended to include a series of experiments with these models in position, these experiments have not been concluded in time for this report.

Figure 6.8 shows a sequence of video photos for ignition in the south goaf (PT .5 of 6.8). Each photograph in the sequence corresponds to a 40ms elapsed time. Flame expands radially from the goaf reaching 27 c/t between 120ms and 160ms. The flame then progresses slowly into No.3 Belt Road and No.4 Supply Road. At the same time (240-280ms) flame rapidly moves along 26 c/t from the south goaf and back towards the goaf along No.3 Belt Road and No.4 Supply Road. On the video it is clear that the flame from the two opposite directions pass through each other in both No.3 Belt Road and No.4 Supply Road.

Between 260ms and 400ms flame is travelling along No.2 Transformer Road towards 25 c/t. The flame then goes both ways along 25 c/t. The northern leg produces a flow towards the goaf along No.3 Belt

Road (440ms) while the southern leg produces a flow back into the goaf along Nos.1 and 1A South Return Roads (440-460ms) reigniting the goaf in the process. It should be noted that residual burning occurs at the corner of 25 c/t and No.1A South Return Road (600ms). The stopping at 26 c/t between No.1 South Return Road and No.2 Transformer Road failed but not the others on the north side.

These results show that the general flow is from south to north and that this ignition does not simulate:

. A flow from No.4 Supply Road toward No.3 Belt Road along 26 c/t. This flow is required to account for both shuttle car positions (see section 6.2.3).

. The direction of flow in No.1A South Return Road and a very strong flow at 440m, is opposite to that observed.

. The strong directional movement of objects from the crib room area along No.4 Supply Road towards 25 c/t. Flow indications are that the flow is generally towards the goaf.

Figure 6.9 shows a similar sequence of video photographs taken after ignition occurred at point 2, the intersection of 27 c/t and No.4 Supply Road. 40ms after ignition, flame has almost reached the position of the mine rover. After 80ms a strong flow develops along No.4 Supply Road moving outbye and 26 c/t moving towards No.3 Belt Road. At 120ms the complete model is covered with flame except for No.1A South Return Road. Flame has extended along 26 c/t and 27 c/t into the goaf. It was difficult to tell from the videos which way the flow moved along No.3 Belt Road. At 160ms residual burning occurred in the crib room while flame was moving out from the goaf area into No.1A South Return Road. This flow continued until after 240ms moving along 25 c/t towards the belt roadway. Residual burning occurs at the corner of No.1A South Return Road and 25 c/t about 280ms.

These results simulate:

. A flow along No.4 Supply Road capable of moving objects in an outbye manner.

. A flow from No.4 Supply Road toward No.3 Belt Road along 26 c/t. This can account for both shuttle car positions.

. The direction of flow along No.1A South Return Road is in the correct direction with no reverse flow observed and a relatively long residence time for flame at the junction with 25 c/t that could account for the fire and high devolotization of coal dust observed in this position.

. The direction of flow along 25 c/t is also consistent with the bending of the belt structure towards the north.

. The flow along 27 c/t from No.4 Supply Road is also compatible with tipping the MPV tray in this c/t.

There is apparently no conflict with the evidence observed at the mine although factors such as the likely movement of objects out of the crib room cannot be determined from this experiment without more details of the pressure and velocities obtained.

In Figure 6.10, the sequence of photographs shows ignition from point 3, the intersection of 26 c/t and No.3 Belt Road. The explosion initially propagates radially from the point of ignition before moving more rapidly into the goaf and down No.3 Belt Road towards the goaf at about 80ms. By 120ms the explosion covers the majority of the mine except for No.1A South Return Road and No.4 Supply Road between 26 c/t and 25 c/t. The direction of movement along 27 c/t and 25 c/t is from No.2 Transformer Road towards the north. At 160ms flame starts moving into No.1A South Return Road from 25 c/t reaching the goaf about 240ms.

These results of this simulation do not agree with the following:

. A flow from No.4 Supply Road towards No.3 Belt Road along 26 c/t, required to account for the unusual position of the shuttle cars.

. The direction of flow in No.1A South Return Road is in the reverse direction to that observed.

. There is not a particularly strong flow outward along No.4 Supply Road needed to move objects from 26 c/t towards 25 c/t.

. The direction of flow along 27 c/t would tip the MPV tray in the wrong direction.

The results however, are consistent with:

. The movement of the belt structure at 25 c/t.

. A long residence time for flame in No.1A South Return Road which could account for the fire and high devolatilisation.

6.6 Computer Simulation Experiments

A number of computer simulations were undertaken in part of the Main dips section of Moura No.4 Mine. The simulations were two dimensional and the area between 27 c/t and 26 c/t and No.3 Belt Road and No.4 Supply Road as depicted in Figure 6.11 was grided on a 0.5m grid. The mine rover, continuous miner, shuttle cars and belt structures were included as fixed structure in the calculation.

The initial conditions in the model assumed an even distribution of fuel, zero velocity and atmospheric pressure throughout the simulation domain. Ignition

is described by a 10% reduction in fuel at one or more cells. This corresponds to a strong ignition source over one cell or a number of cells. One cell describes a weak ignition at a specific site while reduction over a number of cells simulates a much stronger and more extensive ignition. For example, an explosion moving onto the computational domain from the goaf would be simulated by a line of cells corresponding to the width of the roadway at the boundary, while ignition by an electrical arc would be simulated by one cell.

The boundaries on the computational domain simulates either wall or an open boundary. The open boundary will automatically allow flow into or out of the domain depending on the physical conditions existing immediately inside the boundary.

In the simulation, the Pressure, Temperature and Velocities were computed at the points shown in Figure 6.11. The different ignition points are also shown in this figure.

Figures 6.12 to 6.14 show the pressure, velocity parallel to No.4(u) and velocity perpendicular to No.4(v) for ignition at the intersection of 27 c/t and No.4 Supply Road. A positive u velocity corresponds to movement along No.4 Supply Road away from the goaf. A positive v velocity corresponds to movement from No.3 Belt Road towards No.4 Supply Road. In this simulation the stopping at 26 c/t is present and all the vehicles and conveyor are in the positions shown in Figure 6.12.

The time histories of 4 points are shown in Figures 6.12 to 6.14 corresponding to points 10, 7, 2 and 3.

The first pressure peak at point 10 corresponds to a strong combustion wave moving outward (+u) at 28m/s followed by a second peak at about 42m/s moving in the reverse direction. The v velocity oscillates indicative of circulating flows moving past a point. Comparison with a similar experiment without the stopping at 26 c/t being present show that subsequent peaks in the pressure are due to reflections from the stopping. The second pressure peak is due to reflection from the mine rover.

At point 7 the first pressure peak corresponds to a strong outward flow and the second peak is a reflection. The third peak is a reflection from the stopping and is absent when there is no stopping with a high flow towards No.5 North Return Road. Subsequent reflection of different surfaces leads to a complex pattern of peaks.

This complexity is also found in the physical model. Figure 6.15 shows the pressure at this intersection for the same ignition conditions although this corresponded to an 8.3% methane air mixture as opposed to a 9.4% methane air mixture. The ignition source is also much weaker than that simulated in the computer experiment, hence the lower pressures and longer timescales for the physical model experiments. At point 3, the first peak is 50% higher than that at point 7 and corresponds to a very intense flow along 26 c/t from No.4 Supply Road(v). This strong flow also set up an outward flow (+u) along No.3 Belt Road due to the obstruction of the two shuttle cars. The second peak is due to a reflection from s/c No.30 in 26 c/t.

The pressure curve is complex at point 2, due to multiple reflections from the continuous miner and shuttle cars. The initial direction is towards the goaf (-u) while the second series of pressure peaks after 84m seems to be due to reflection from the continuous miner. The transverse velocity oscillates wildly, again indicative of vortex formation.

Figures 6.16 to 6.18 show the pressure the velocities for an ignition in 9.4% methane air mixture at the intersection of 26 c/t and No.3 Belt Road.

Point 3 is nearest to the ignition point and the pressure is the lowest of those shown but still displays a complex pattern due to reflections off nearby surfaces. Both the u and v velocities fluctuate due to these reflections. At point 2 the flow is towards the goaf (-u) with reflection from the continuous miner.

At point 7 the initial pressure pulse and combustion wave move towards the stopping away from the shuttle cars along 26 c/t. The second peak is a reflection from the intersection sides of the mine rover and moves in the +u direction.

At point 10 the pressure pattern is complex with the initial peaks corresponding to movement into the goaf with strong transverse oscillation.

Both sets of simulation corresponds to detonation in the mine. As such they are unrealistic simulations of this incident. The reason for the high pressure, velocities and temperature observed could be due to a number of reasons:

- The time frame required for this report did not allow proper calibration of the model against known benchmarks. As a consequence some of the parameters could be improperly prescribed or there could still be an error in the code.

- The ignition description corresponds to an extensive ignition source particularly for the case where a number of cells are prescribed to cover an ignition source. This could have lead to overdriving the accelerative process in the model leading to rapid detonation. An alternative description of ignition with laminar conditions and an induction delay, typically observed for a weak ignition source has not as yet been added to the model.

- This model couples the reaction rate to the levels of turbulence. This coupling originally caused numerical instabilities in the sequential version of this code which were overcome. The corrections, to the code were included in the parallel code used for these simulations but the more complex geometrics could still cause unrealistic turbulence levels and hence two high a reaction rate.

Further work is required to calibrate the model. There are two relevant benchmarks against which this model can be tested. Professor Hjertager has used his simulation model against a 10m ignition tube problem. In discussion with him it was agreed to use this as one benchmark against which both

explosion codes could be tested and developed further. The second benchmark is that of a detonation of gas in a shock tube. Experiments by Lee can be used as the basis for this benchmark. The reason for using both a supersonic and subsonic benchmark is to test whether these are constraints on the use of the code.

Further work is also required to assess alternative strategies for coupling the chemical kinetics into the model. Discussion on this point with Drs Oran and Hjertager highlights two alternative approaches. In one the chemistry is decoupled from the turbulence. A single Arrhersius reaction rate is used for the chemical source term. This would normally lead to overprediction of the reaction rate but this can be overcome by averaging the temperature field for the cell where reaction rate is being calculated. In the second approach, the chemistry remains coupled to the turbulence but severe restraints are imposed on the growth of turbulence. This has the advantage that it is empirical and easy to implement and would be suitable for flows where there is plenty of obstacle generated turbulence. It has disadvantages when there are few obstacles and requires recalibration for different types of problems.

It is also suggested that the scale model be used to calibrate the computer model for the Moura explosion in further work. The calibrated model can then be used to assess alternative hypothesis for the Moura explosion.

Computer simulation is the only method by which details of flow and combustion can be predicted for an explosion in a cost-effective manner. Physical modelling will give an insight into what is occurring but even sophisticated and costly laser diagnostic techniques are not fast enough to obtain information on velocities, turbulence and chemistry in a fully developed explosion. Such techniques are difficult to use even in steady non-combustion flows.

There is, however, a need to calibrate and validate the computer code. This was not possible in the time frame for this report but the technique highlights its potential use for forensic studies in the future:

- The ability to determine the pressure field with time for every point in the domain of computation. The impulse can be estimated directly from these calculations. Theories on the movement or deformation of objects in an explosion can readily be assessed.

- The ability to determine the temperature field with time for any point. The heat load can be estimated for any material surface from these calculations and the likely heat damage can readily be assessed for a given explosion.

6.7 Discussion

The use of modelling has shown their potential in assisting with understanding what occurs in a mine explosion. For example the physical modelling undertaken to date has shown that the only way of obtaining a one way flow along No.1A South Return Road is with a relatively strong explosion travelling through the south goaf from 27 c/t. The flow ahead of this type of explosion

seems to prevent even a strong explosion moving along 25 c/t toward No.1A South Return Road from the wrong direction to that observed. Such an explosion is forced along No.1 South Return Road towards the goaf. A weak explosion along 27 c/t into the south goaf area does not show the same trend. To date, only two ignition points have given a flow in the correct direction at No.1A South Return Road and that is from the intersection of 27 c/t and No.4 Supply Road and from the crib room.

Much more work is required, however to say that these are the only ignition areas in the mine that can simulate the observed effect. Similarly the mathematical modelling with computers has the potential to accurately simulate the flow around obstacles, the reversal in flows, the pressure and impulses on objects and elucidate the observations following an explosion. Much more work is required to develop this method as it has many applications for hazard assessment and control in the mine environment apart from its application to investigation.

TABLE 6.1 PRESSURE DAMAGE FROM CHEMICAL AND NUCLEAR EXPLOSION

OVERPRESSURE ;psi	;kPa	DAMAGE
0.03	0.2	Occasional breaking of large glass windows already under strain.
0.1	0.7	Breaking of small windows already under strain.
0.15	1.0	Normal limit for glass breakage.
0.25	1.7	50% window glass breakage.
0.3	2.0	>10% window glass broken. Some damage to house ceilings Missile limit "Safe distance" (0.05 probability of no serious damage beyond this limit).
0.4	2.8	Limited minor structural damage.
0.55	3.8	90% window glass breakage.
0.5-1.0	3.5-7.0	Large and small windows usually shattered and occasional damage to window frames.
0.7-0.75	4.8-5.0	Minor damage to house structures. 20-50% tiles displaced and breakage of small windows not under strain.
0.9	6.2	Roof damage to oil storage tanks. Branch damage to trees.
0.9-1.0	6.2-6.9	Nearly all window glass broken.
1.0	6.9	Partial demolition of houses, made uninhabitable.
1.0-1.5	6.9-10.3	Branch damage to trees. Asbestos cladding blown off buildings.
1.0-2.0	6.9-13.8	Asbestos cladding shattered. Fastenings of corrugated steel and aluminium panels fail and panels distorted. House tiled roof lifted and replaced.
1.3	9.0	Steel frame of clad buildings slightly distorted.
<1.5	<10.3	Houses lightly damaged (Category D damage), but remain inhabitable after repair.
1.5	10.3	Most window glass broken, but only light damage to window frames and doors. Moderate plaster damage. Most tiles displaced, but laths intact.
1.5-6.0	10.3-41	Houses severely to moderately damaged (Category C damage).
2.0	13.8	Partial collapse of walls and roofs of houses. Load bearing brickwork unaffected 30% trees blown down.
2.0	13.8-17.2	Some frame distortion of steel girder framed buildings.
2.0-3.0	13.8-20.7	Concrete or cinder block walls (8-12" thick, but not reinforced) shattered. Deflection of steel posts.
2.3	15.9	Lower limit of serious structural damage.
2.5	17.2	50% destruction of house brickwork, rafters and laths broken.
3.0	20.7	90% trees blown down. Steel framed building distorted and pulled away from foundations. Heavy machines (3000 lbs) suffer little damage. Frameless, self-framing, steel panel buildings demolished.
3.0-4.0	20.7-27.6	Rupture of oil storage tanks. Collapse of self-framing steel panel buildings.
3.5	24.1	Oil storage tanks distorted.
3.5-4.5	24.1-31	Collapse of steel posts.
4.0	27.6	Cladding of light industrial buildings ruptured.
4.0-5.0	27.6-34.5	Severe displacement of motor vehicles.
4.5	31	Severe distortion to frames of steel girder framed buildings.
5	34.5	Wooden utility poles snapped.
5-7	34.5-48	Nearly complete destruction of houses.
6-8	41-55	Houses irreparably damaged (Category B damage).
7	48	Loaded rail cars overturned.
7-8	48-55	Brick panels (8-12"), but not reinforced fail by shearing or flexure.
7-9	48-62	Collapse of steel girder framed buildings.
7-10	48-70	Cars severely crushed.
8-9	55-62	Brick walls severely cracked.
8-10	55-70	Brick walls completely demolished.
9	62	Collapse of steel truss type bridges. Loaded train box-cars completely demolished.
>10	>70	Total destruction of houses (Category A damage) and most buildings. Heavy machine tools (7000 lbs) moved and badly damaged. Very heavy machine tools (12000 lbs) survive.
13	90	18" brick walls completely destroyed.
17	120	Oil storage tanks completely destroyed.
20	140	Virtually complete destruction of all buildings, other than reinforced concrete aseimic designs.
70	480	Collapse of heavy masonry or concrete bridges.
280	2000	Limit of crater lip.

Sources: Astbury [53], Brasie [54], Clancy [55], Glasstone [56,57], Health & Safety Commission [58], Home Office [59], Jenett [60], Roberts [61].

Table 6.2 Maximum and Minimum movement of brick debris

Velocity	P	t_d = 100ms			t_d = 200ms			t_d = 400ms			t_d = 600ms		
		d_{Max}	d_{Min}	I	d_{Max}	d_{Min}	I	d_{Max}	d_{Min}	I	d_{Max}	d_{Min}	I
	Bar	(m)	(m)	(kPas)	(m)	(m)	(kPas)	(m)	(m)	(kPas)	(m)	(m)	(kPas)
50	0.22	0.35	0.10	0.145	0.66	0.15	0.29	1.17	0.17	0.58	1.51	0.17	0.87
100	0.48	1.47	0.46	0.580	2.94	0.92	1.16	5.84	1.81	2.32	8.68	2.66	3.48
150	0.78	3.58	1.31	1.305	7.68	3.18	2.61	17.29	8.49	5.22	28.6	15.8	7.83
200	1.13	7.01	3.02	2.320	16.2	8.36	4.64	39.90	25.4	9.28	69.3	49.7	13.92
250	1.53	12.2	6.07	3.625	30.0	18.3	7.25	77.4	57.5	14.50			
300	1.99	19.7	11.06	5.220	50.4	34.7	10.44						
350	2.50	30.1	18.60	7.105									
400	3.08	43.7	29.4	9.280									

t_d is the wind duration (msec.)

d is the distance of brick travel

I is the impulse on the brick

Table 6.3 - Damage sustained to brick stoppings

ct	Head	Condition	Projected Outward Distance m	Projected Inward Distance m
27	4/5	Partly gone.	Bricks either side of wall but not to a great distance (<3m).	
26	4/5	Gone: projected mainly towards rib.	7.5-15 (18)*	6-10 (20)*
25	4/5	Gone: majority against rib.	10-23	-
24	4/5	Gone: all against rib.	10-12	-
23	4/5	Gone: projected mainly towards rib. Door moved out 7m.	3-13	-
22	4/5	Partly gone: projected mainly towards rib. Door moved about 2m.	0-10	-
21	4/5	Partly gone: not projected any distance.	0-3	-
25	1/2	Gone: projected in both directions, door moved 7m	12-18 (25)*	0-7 (25)*
24	1/2	Gone: projected mainly against rib. Door moved 18m outward	15-20	- (8)*
23	1/2	Gone: projected mainly against rib.	11-16	- (30)*
22.5	1/2	Gone: projected towards rib.	3-10 (17)*	-
23/ 22.5	2	Gone: projected into water in heading.	10->30	-
23/ 22.5	1	Gone: projected into water in heading.	10->30	-
22	1/2	Intact	-	-
21	1/2	Intact	-	-
20A	1/2	Intact	-	-

* Distance of furthest brick from wall.

Table 6.4 Air Velocities and Impulse based on Maximum and Minimum brick displacements

ct	Heading	Impulse kPas	td = 0.1ms				td = 0.2ms				td = 0.4ms				td = 0.6ms			
			V_{max} m/s	P_{max} Bar	V_{min} m/s	P_{min} Bar	V_{max} m/s	P_{max} Bar	V_{min} m/s	P_{min} Bar	V_{max} m/s	P_{max} Bar	V_{min} m/s	P_{min} Bar	V_{max} m/s	P_{max} Bar	V_{min} m/s	P_{min} Bar
27	4/5	0-1.05	150	0.77	0	0	110	0.52	0	0.	80	0.36	0	0	65	0.28	0	0
26	4/5	4.27-5.21	200	1.13	270	1.71	205	1.17	180	0.18	150	0.77	140	0.70	120	0.58	110	0.52
25	4/5	5.34->6.27	>310	2.10	290	1.90	>220	1.29	210	1.29	>160	0.84	150	0.77	>130	0.65	125	0.61
24	4/5	>5.34	>290	1.90	290	1.90	>210	1.21	210	1.21	>150	0.77	150	0.77	>125	0.61	125	0.61
23	4/5	1.91-4.01	250	1.54	200	1.13	175	0.95	150	0.77	130	0.64	110	0.52	110	0.52	100	0.47
22	4/5	0-3.20	230	1.37	0	0.	155	0.81	0	0.	120	0.58	0	0	105	0.49	0	0
21	4/5	0-1.05	150	0.77	0	1.	110	0.52	0	0.	80	0.36	0	0	65	0.28	0	0
25	1/2	6.09-6.65	340	2.40	325	2.25	240	1.45	230	1.37	170	0.91	165	0.88	135	0.68	130	0.65
24	1/2	>7.04	-	-	345	2.45	-		245	1.50	-	-	175	0.95	-	-	140	0.70
23	1/2	>5.72	-	-	310	2.10	-		220	1.29	-	-	153	0.81	-	-	120	0.58
22.5	1/2	1.91-4.99	295	1.95	200	1.13	205	1.71	150	0.77	145	0.74	110	0.52	115	0.55	100	0.47
22	1/2	0	0	-	-		0		-		0	0	-		0	0	-	-
21	1/2	0	0	-	-		0		-		0	0	-		0	0	-	-

1 Bar = 100 kPa = 15.2 psi

Table 6.5 Movement of Shuttle Car No. 31

Air Velocity	t_d = 0.1		t_d = 0.2		t_d = 0.4		t_d = 0.4	
	d m	I kPas	d m	I kPas	d m	I kPas	d m	I kPas
50	0.00	0.145	0.00	0.29	0.0	0.58	0.0	0.87
100	0.004	0.580	0.02	1.16	0.06	2.32	0.13	3.48
150	0.04	1.305	0.16	2.61	0.65	5.22	1.47	7.83
200	0.15	2.320	0.60	4.64	2.43	9.28	5.48	13.92
250	0.39	3.625	1.58	7.25	6.36	16.50		
300	0.84	5.220	3.40	10.44				
350	1.59	7.105						
400	2.75	9.280						

d is the distance that one end of the shuttle car has moved about the other end.

Table 6.6 Body Displacement

Velocity	t_d = 0.1			t_d = 0.2			t_d = 0.4			t_d = 0.6		
	Displacement SF	SS	I kPas	Displacement SF	SS	I kPas	Displacement SF	SS	I kPas	Displacement SF	SS	I kPas
50	0.06	0.01	0.145	0.15	0.03	0.29	0.38	-	0.58	-	-	-
100	0.69	0.16	0.580	2.03	0.45	1.16	5.73	1.28	2.32	10.6	2.10	3.48
150	2.77	0.68	1.305	8.28	1.98	2.61	24.4	5.64	5.22	95.6	10.3	7.83
200	7.24	1.81	2.32	21.8	5.38	4.64	65.4	15.8	9.28	123	29.2	13.92
250	15.1	3.84	3.625	46.1	11.5	7.25	138	34.2	14.50	263	64.1	21.75
300	27.6	7.05	5.22	84.3	21.3	10.44	-	63.7	20.88			
350	45.8	11.7	7.105									
400	71.0	18.3	9.28									

SF - standing face on

SS - standing side on

FIGURE 6.1

Plot of the position of the dummy during translation as viewed at the side of the vertical plane in which it moved

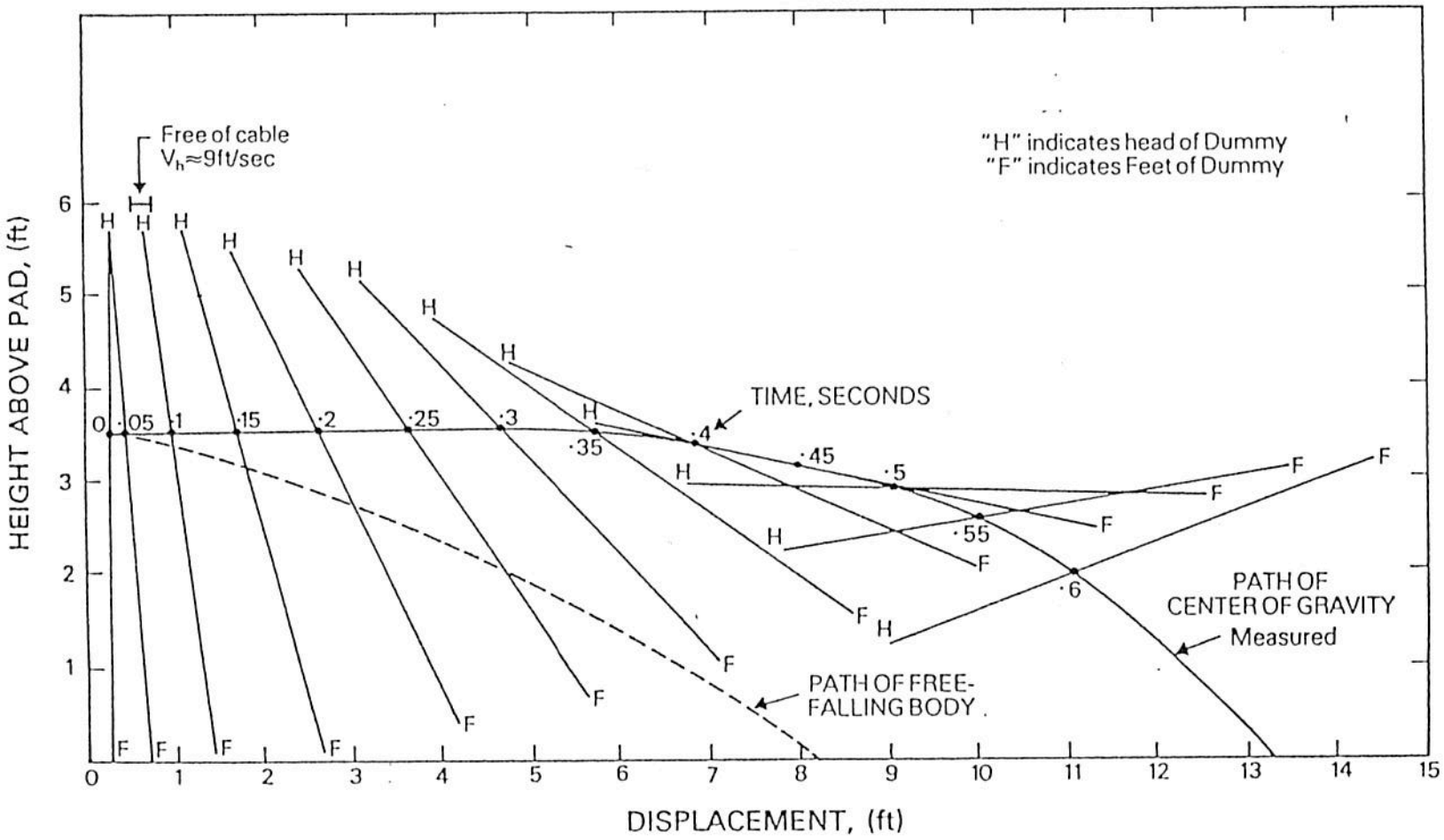

(From Taborelli et al, [40])

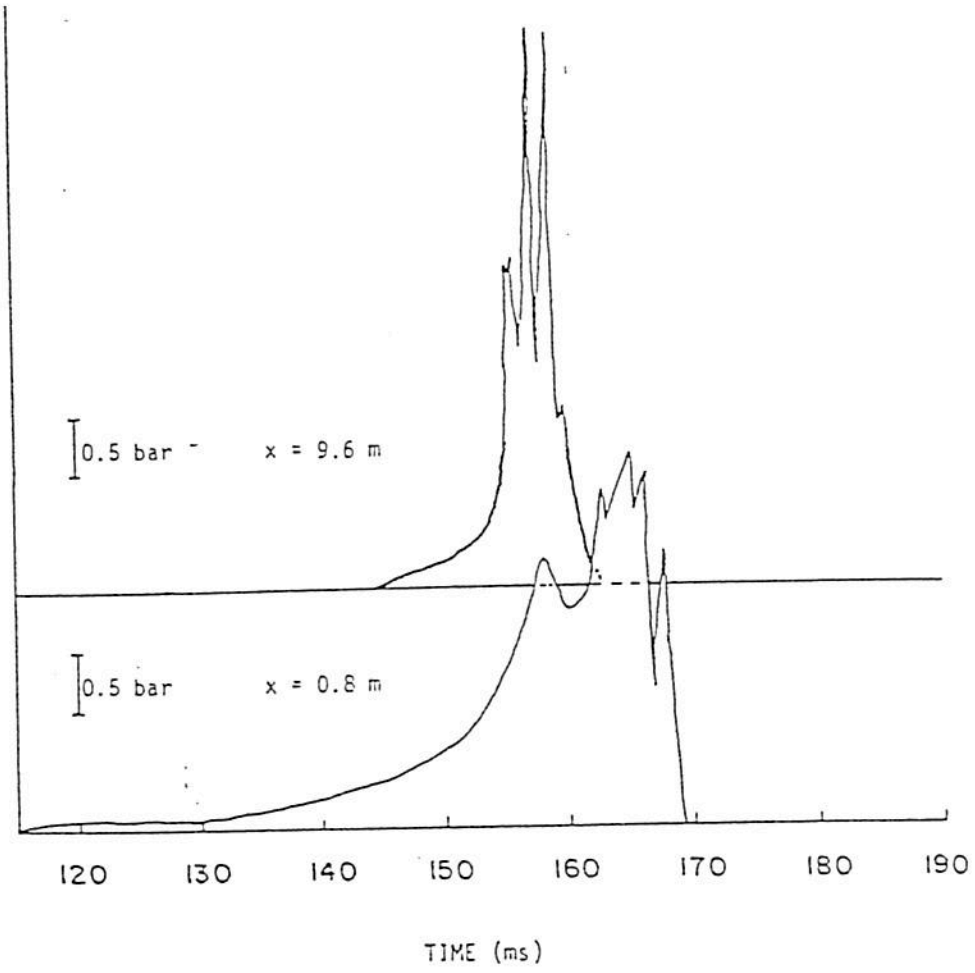

Figure 6.2 10m Ignition Tube - Experimental Pressures.

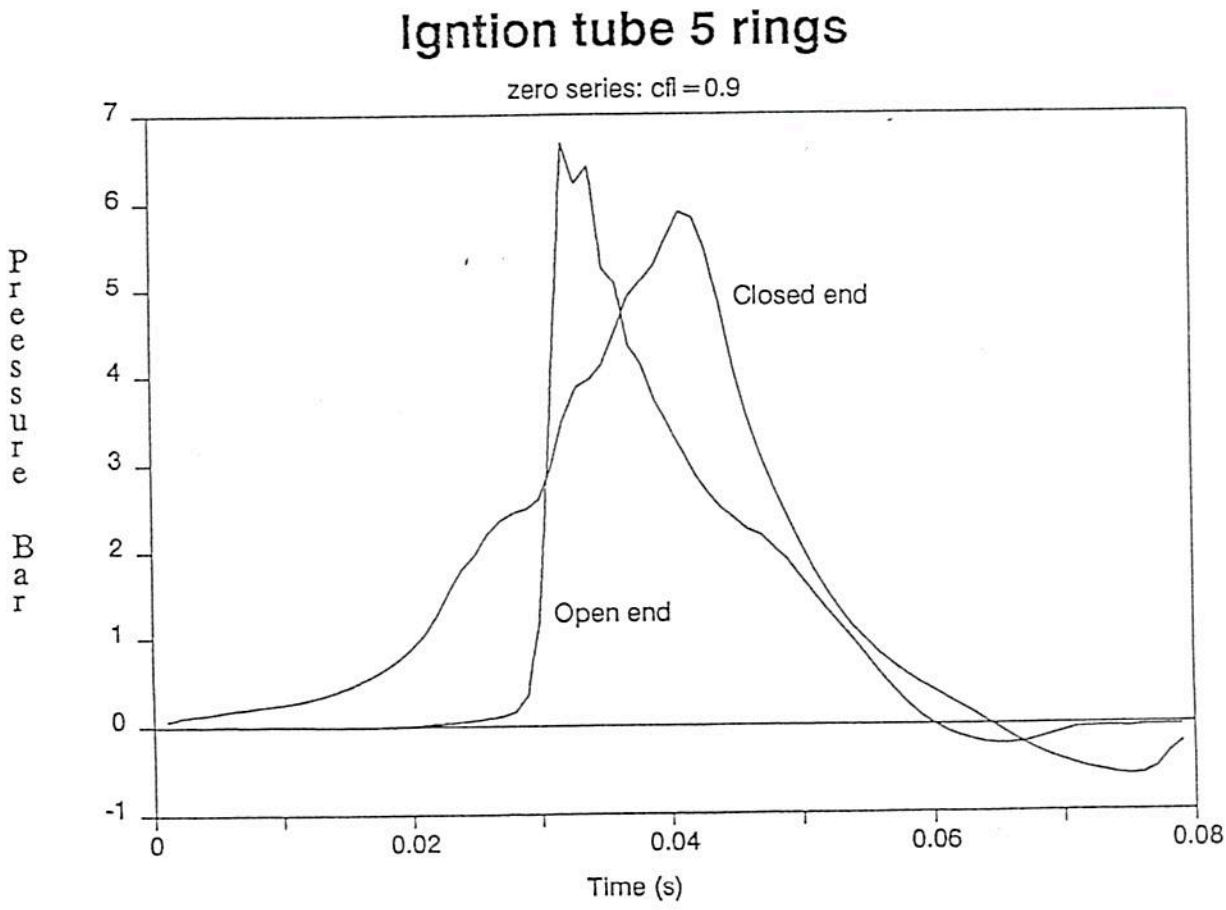

Figure 6.3 10m Ignition Tube - Calculated Pressures.

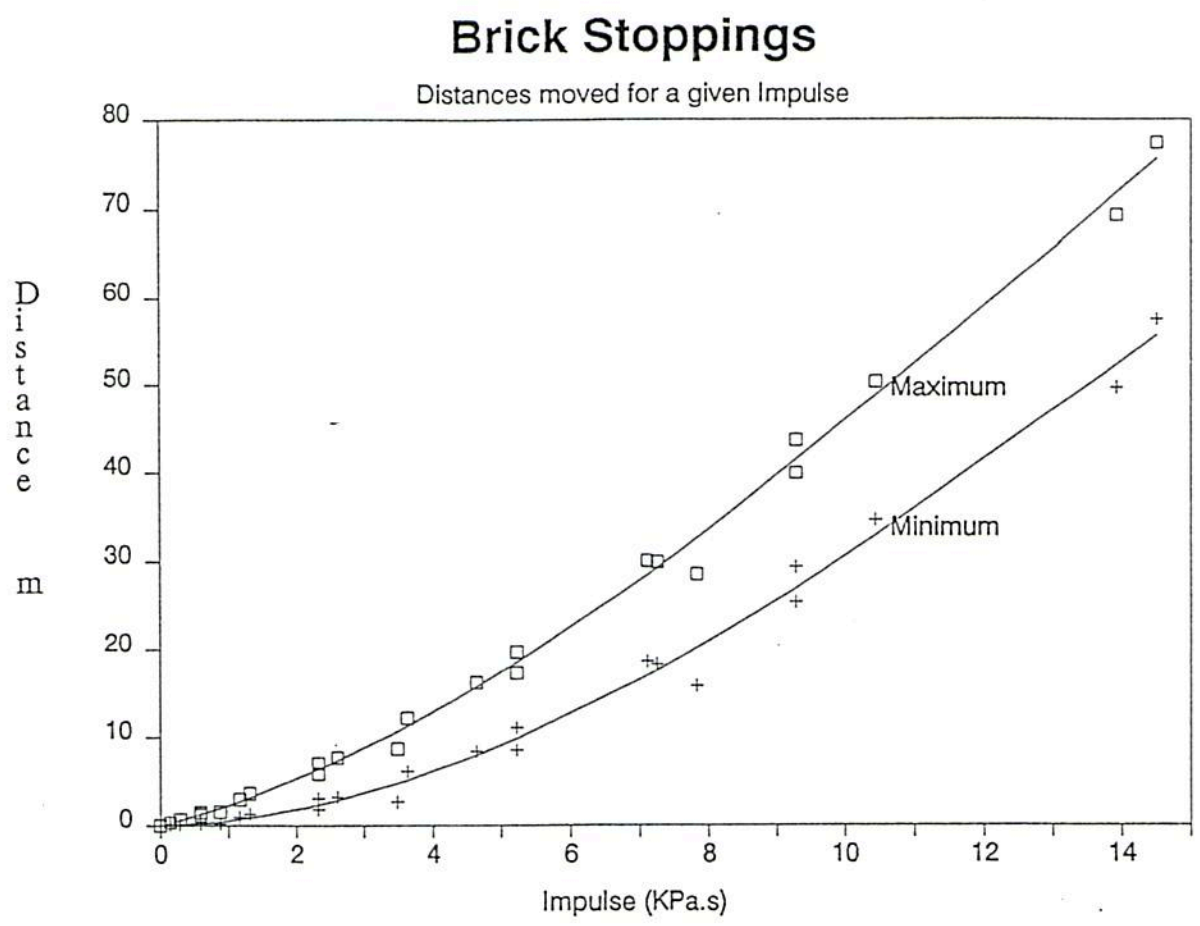

Figure 6.4 Movement of Mine Stopping Debris.

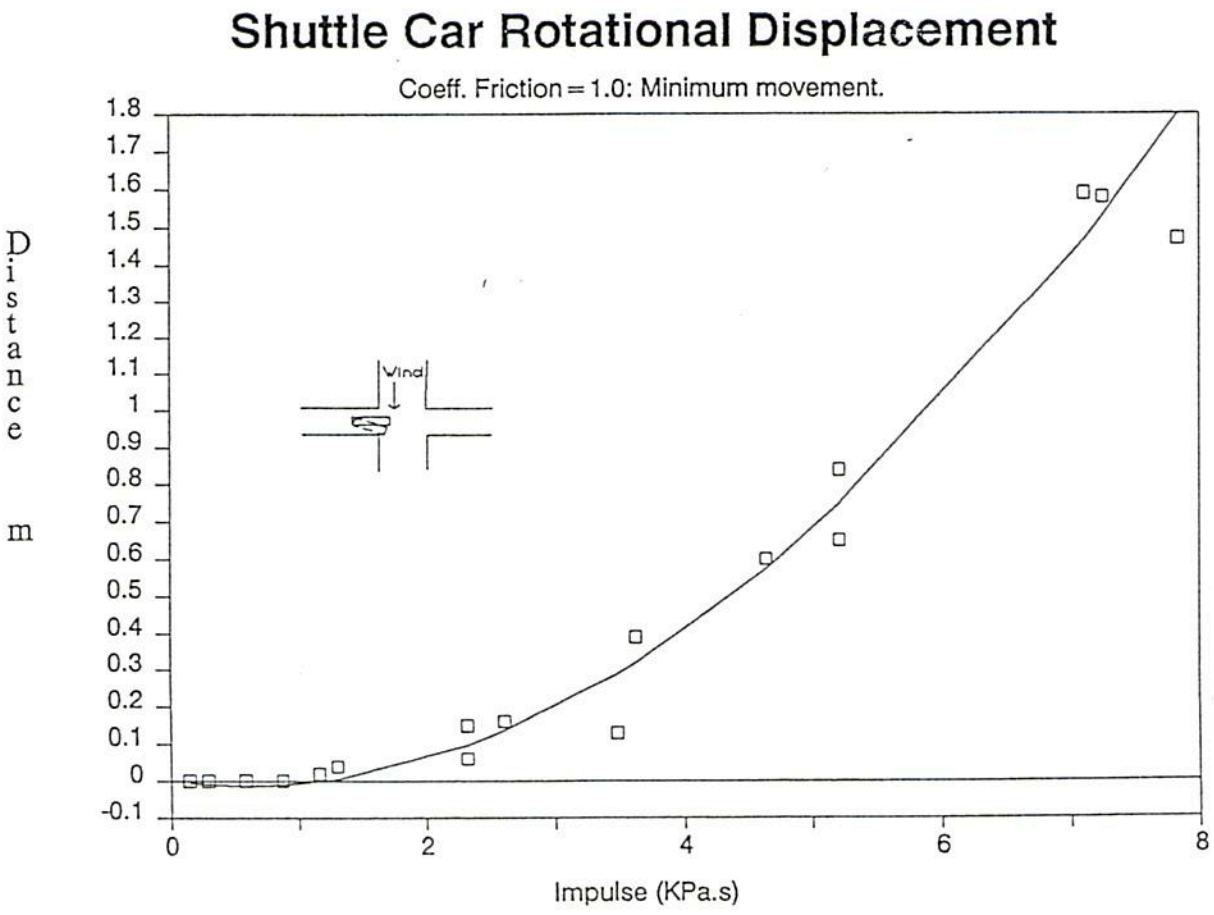

Figure 6.5 End Displacement of Shuttle Car 31

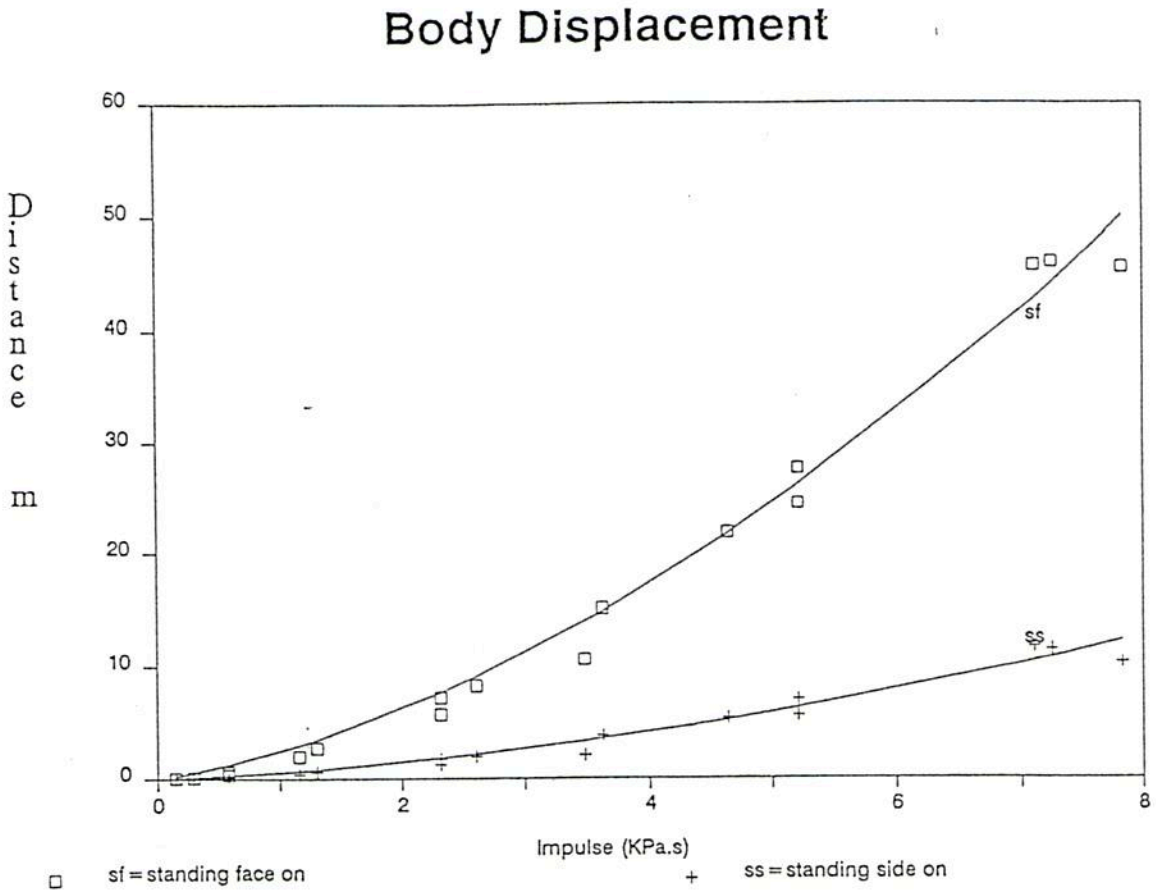

Figure 6.6 Body displacement.

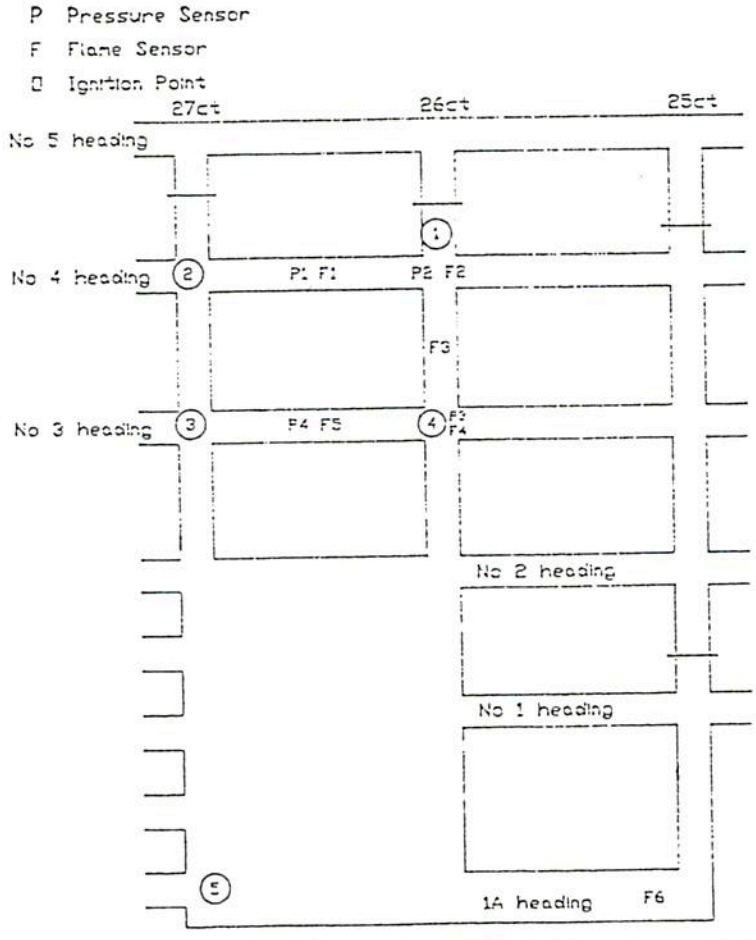

Figure 6.7 Schematic of the 1:54 scale model

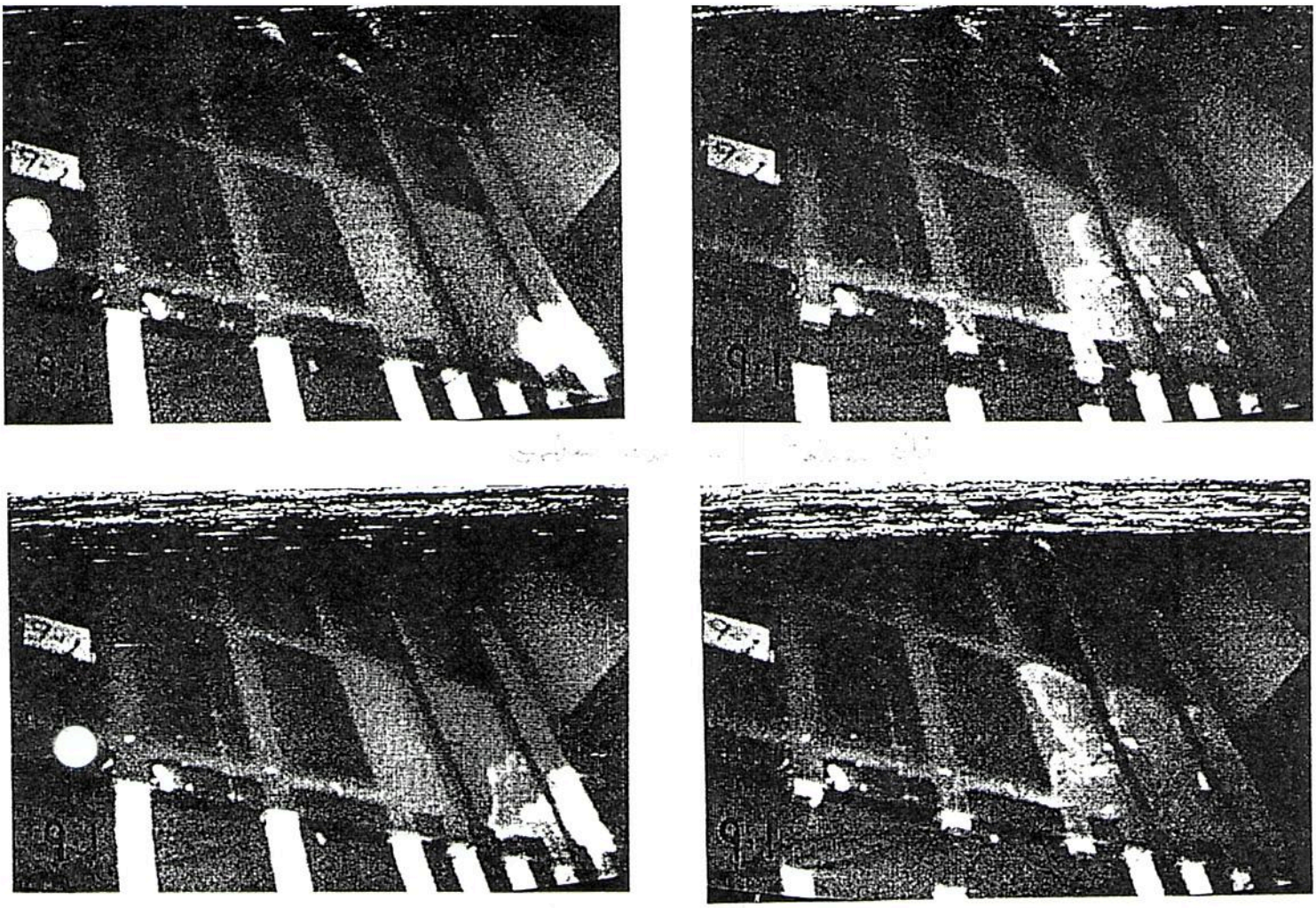

FIGURE 6.8 IGNITION: SOUTH GOAF

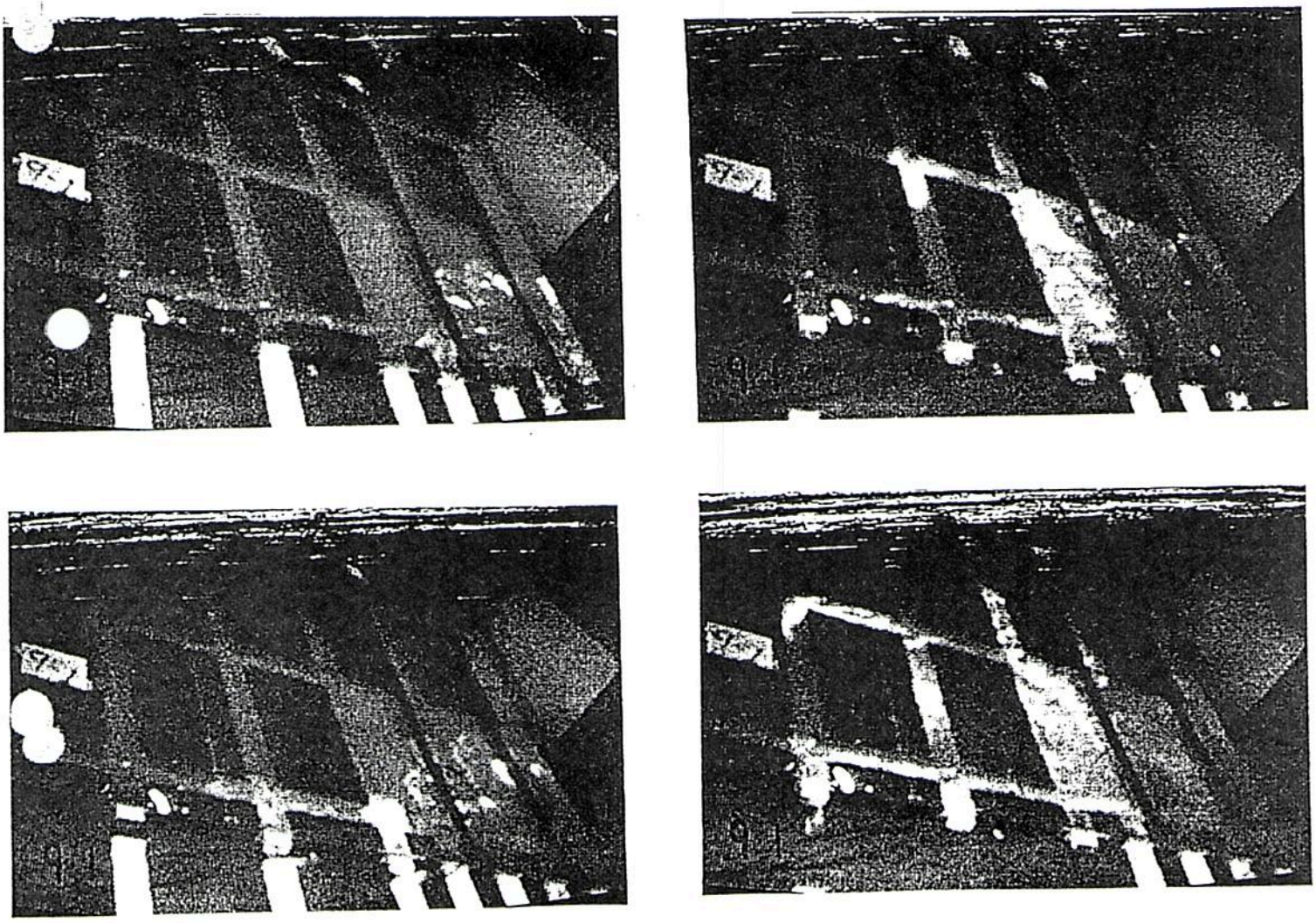

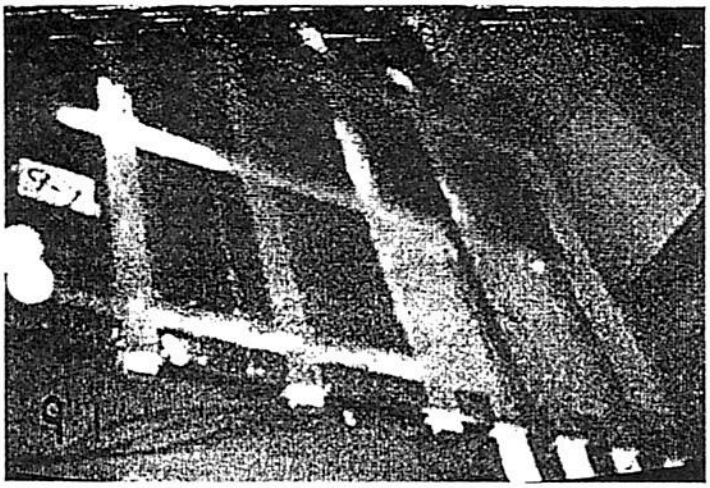

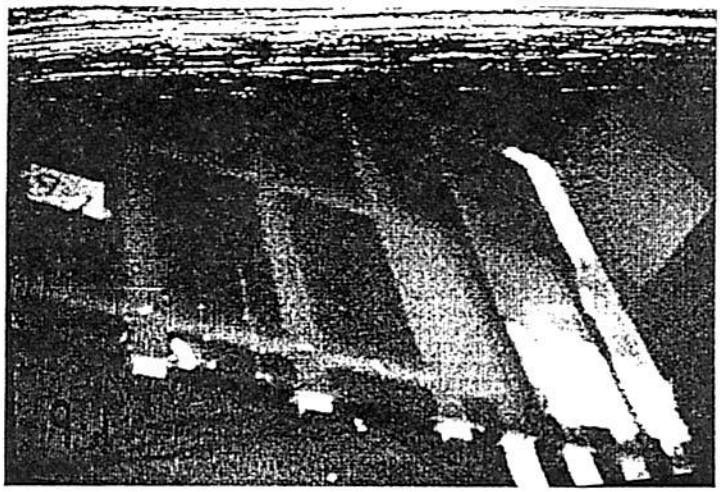

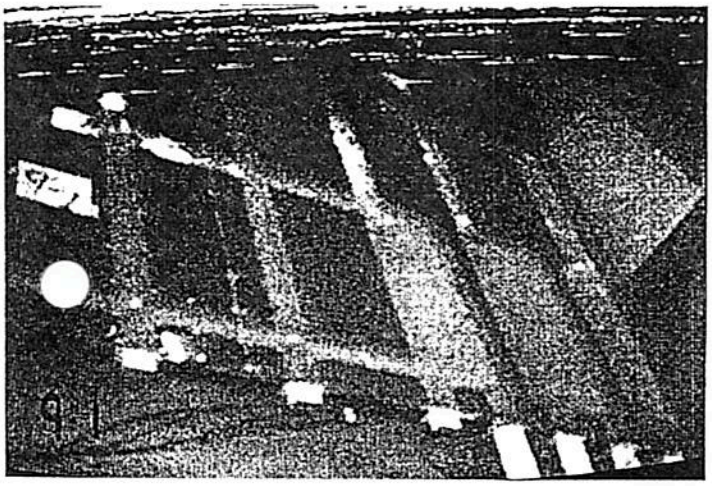

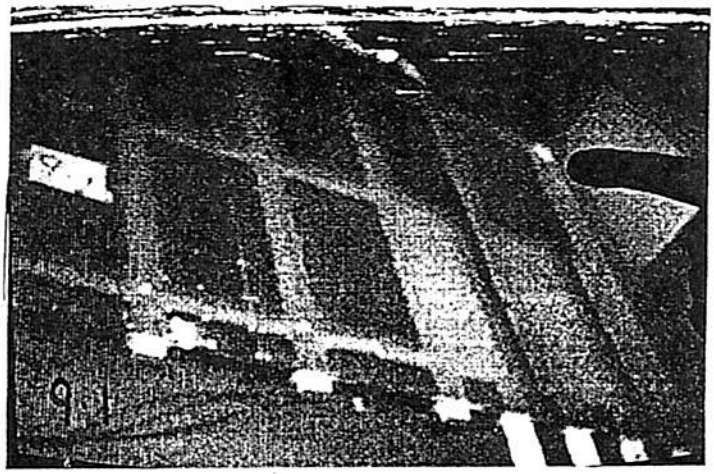

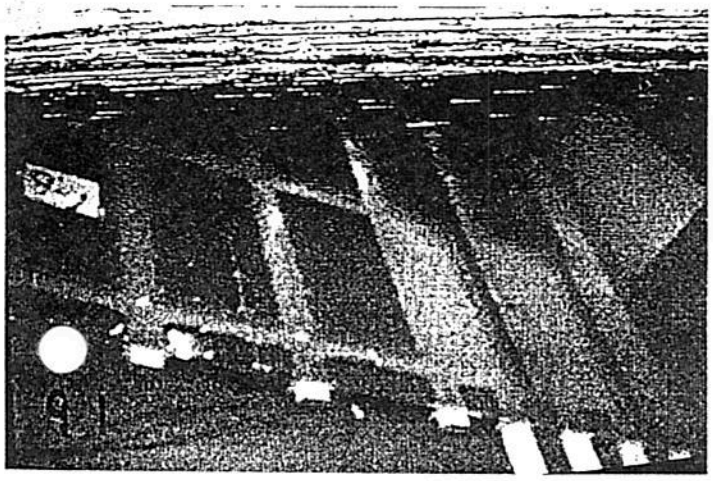

FIGURE 6.8 CONTINUED

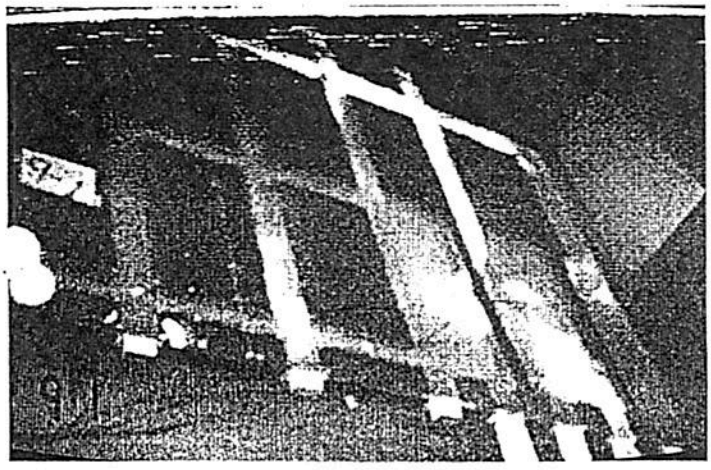

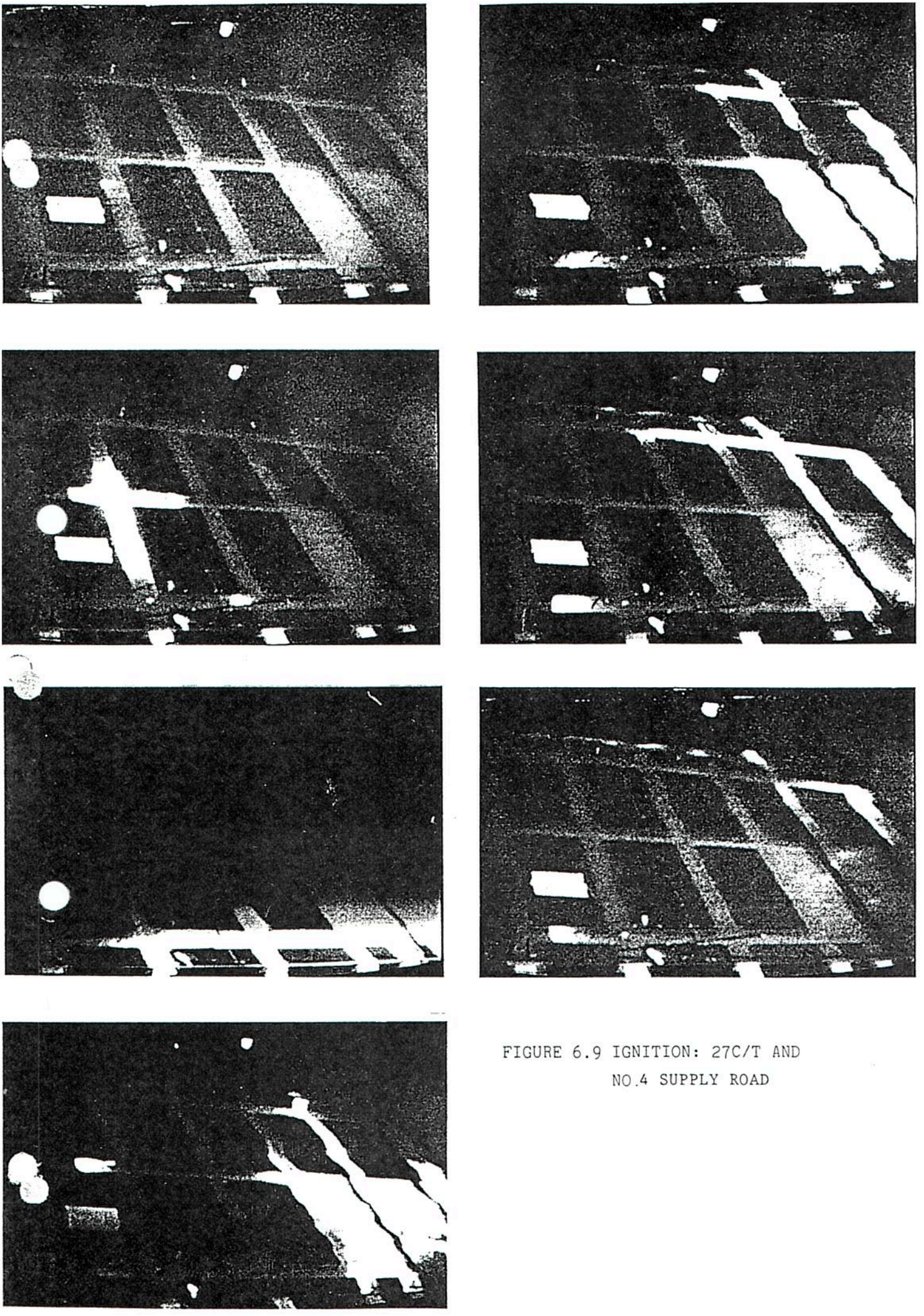

FIGURE 6.9 IGNITION: 27C/T AND NO.4 SUPPLY ROAD

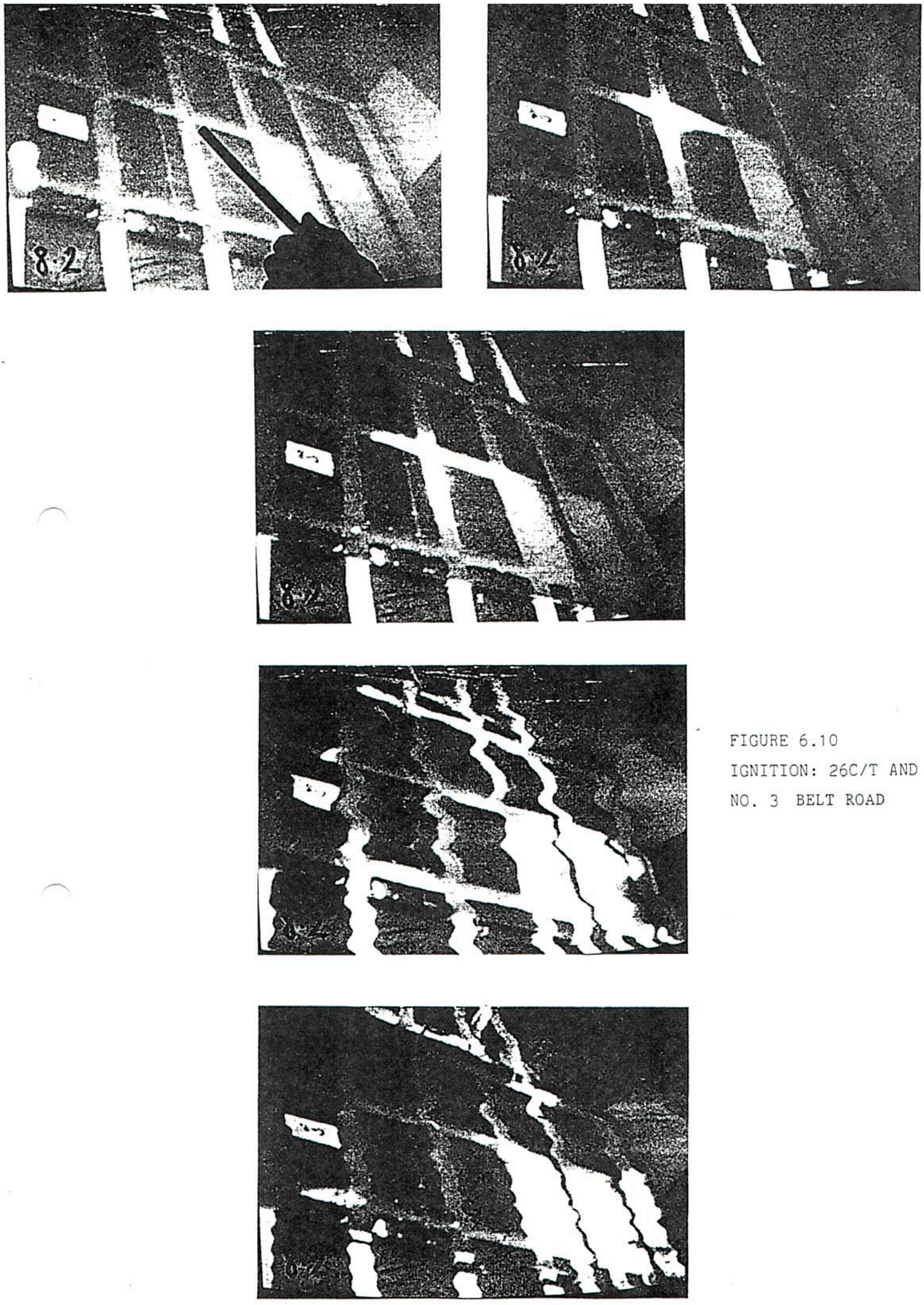

FIGURE 6.10
IGNITION: 26C/T AND
NO. 3 BELT ROAD

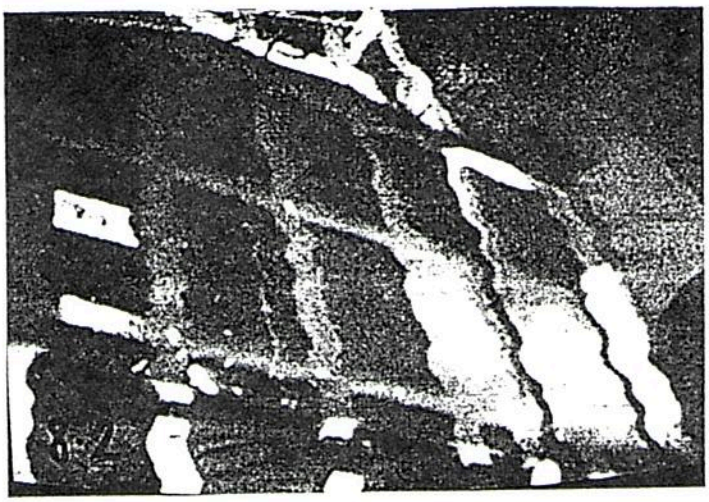

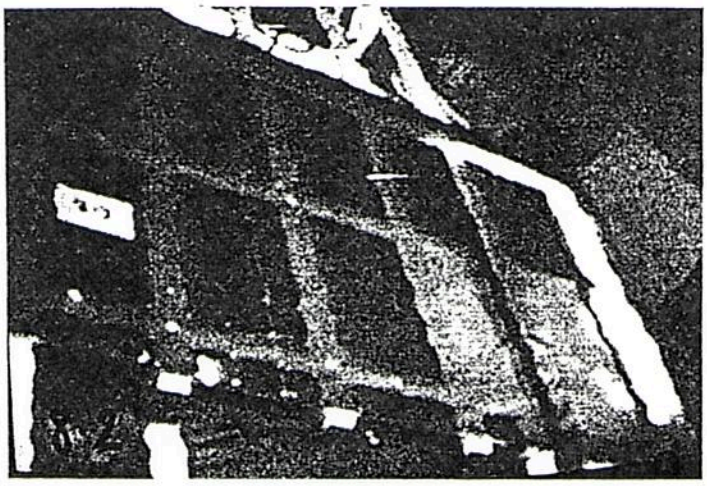

FIGURE 6.10 CONTINUED

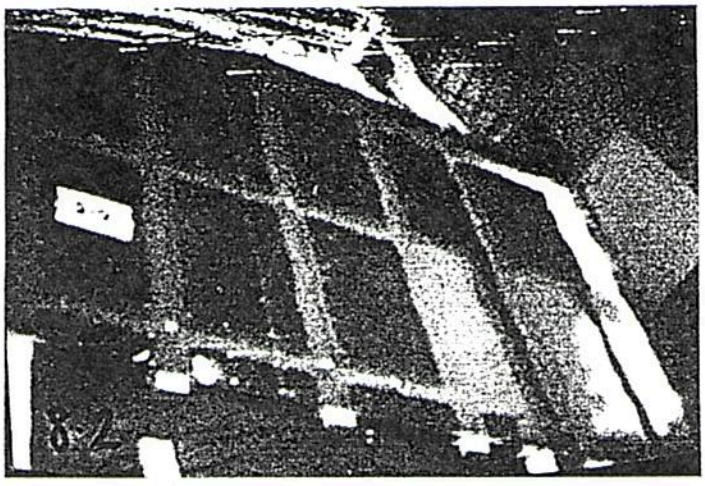

FIGURE 6.11

GRID USED FOR THE MATHEMATICAL
SIMULATIONS: RESOLUTION 0.5M

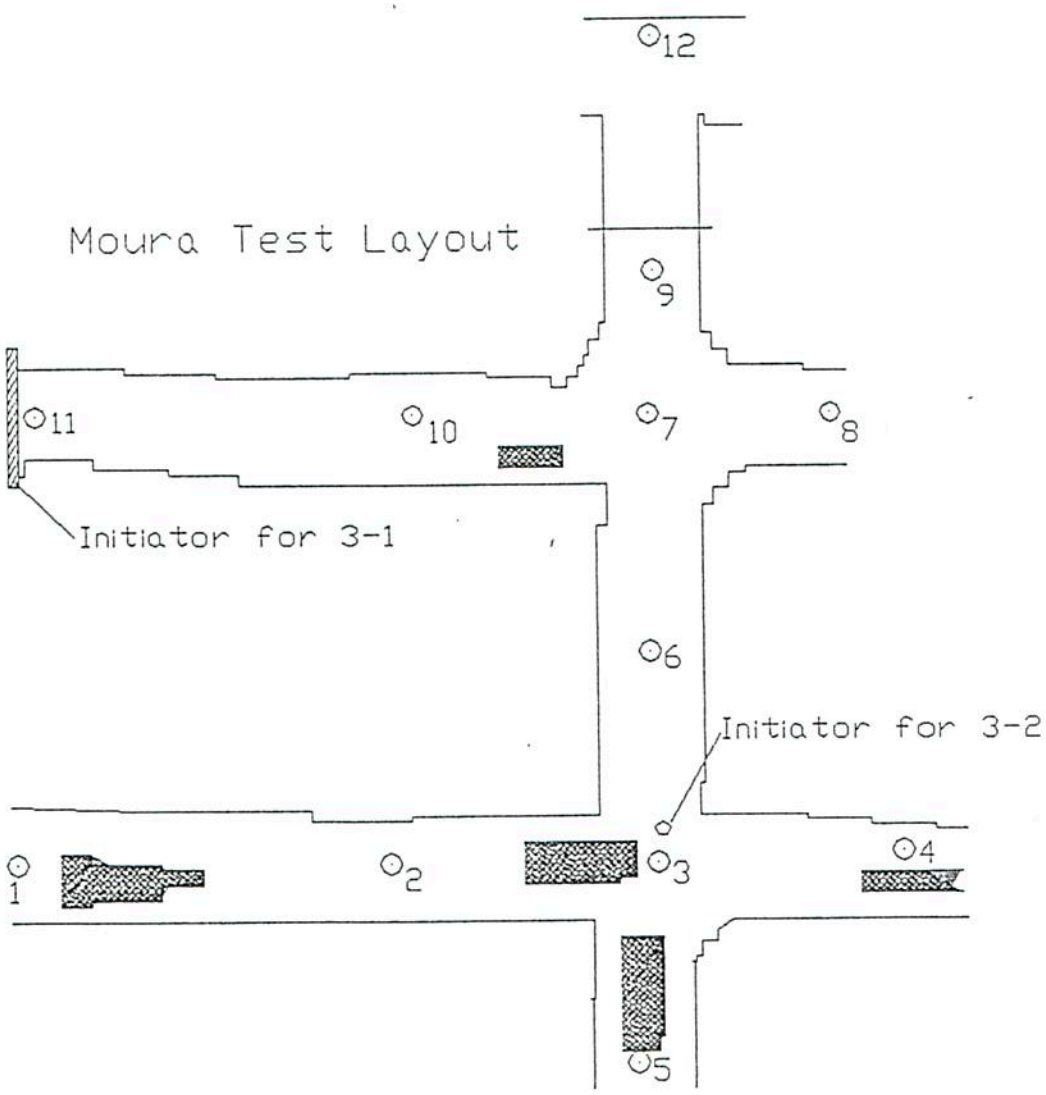

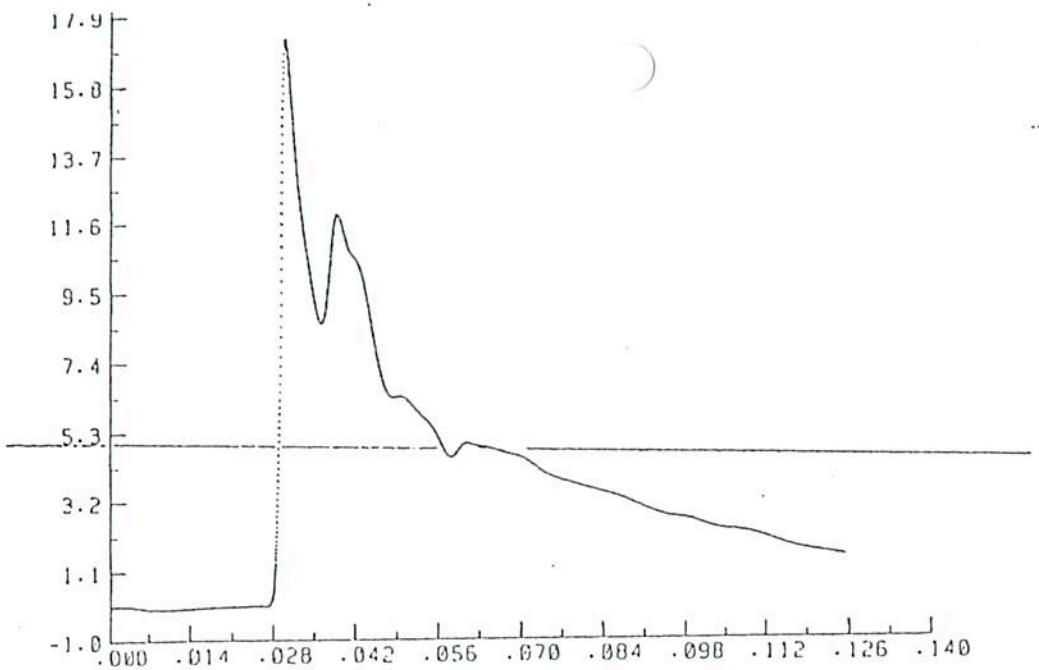

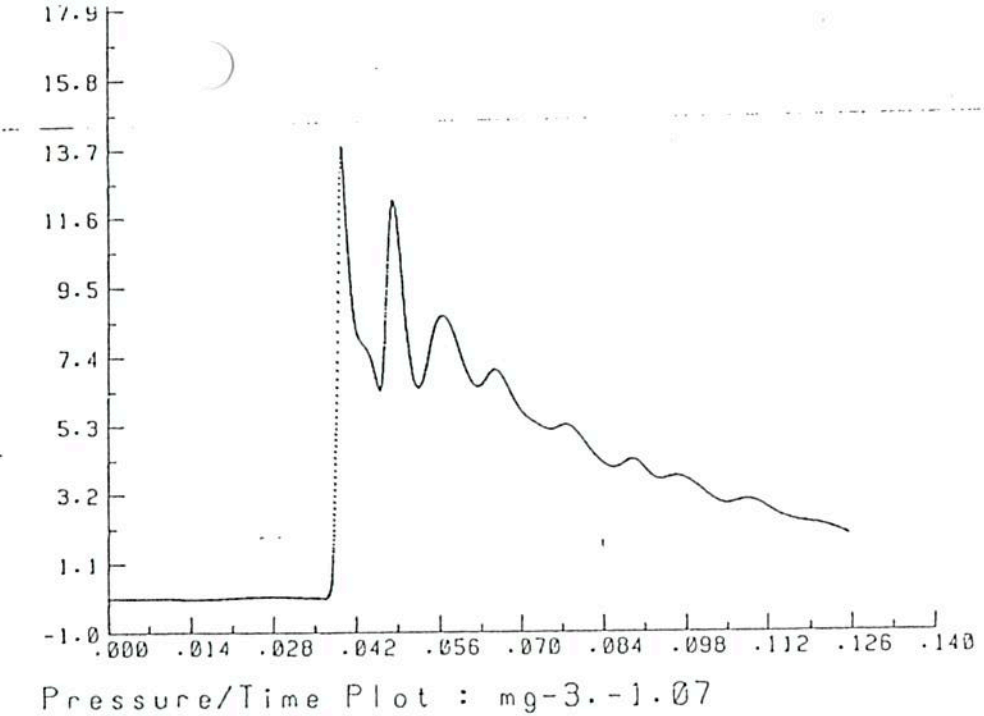

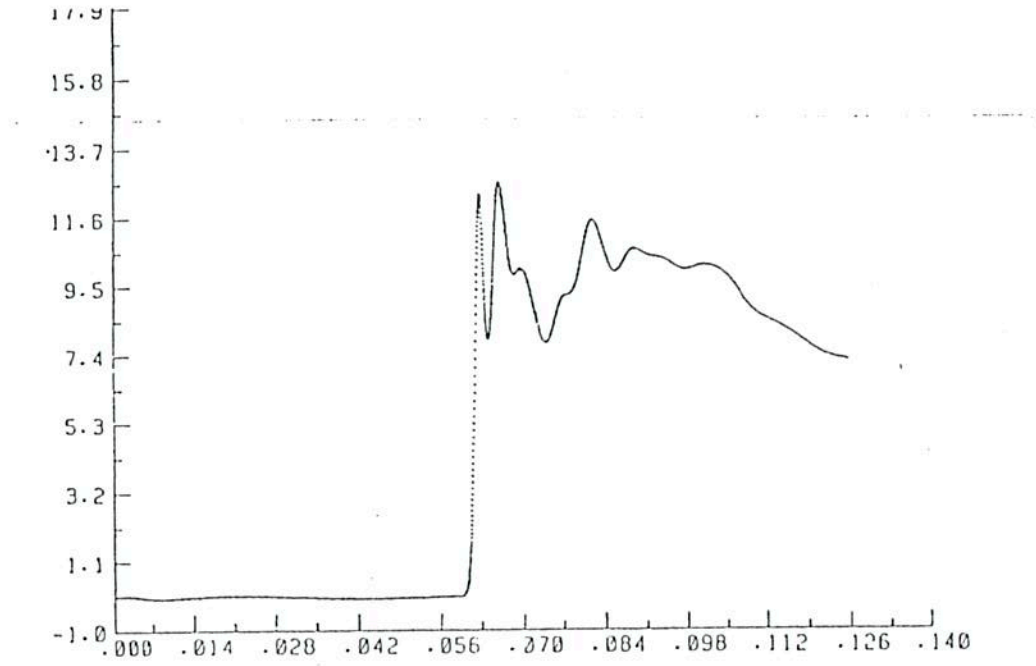

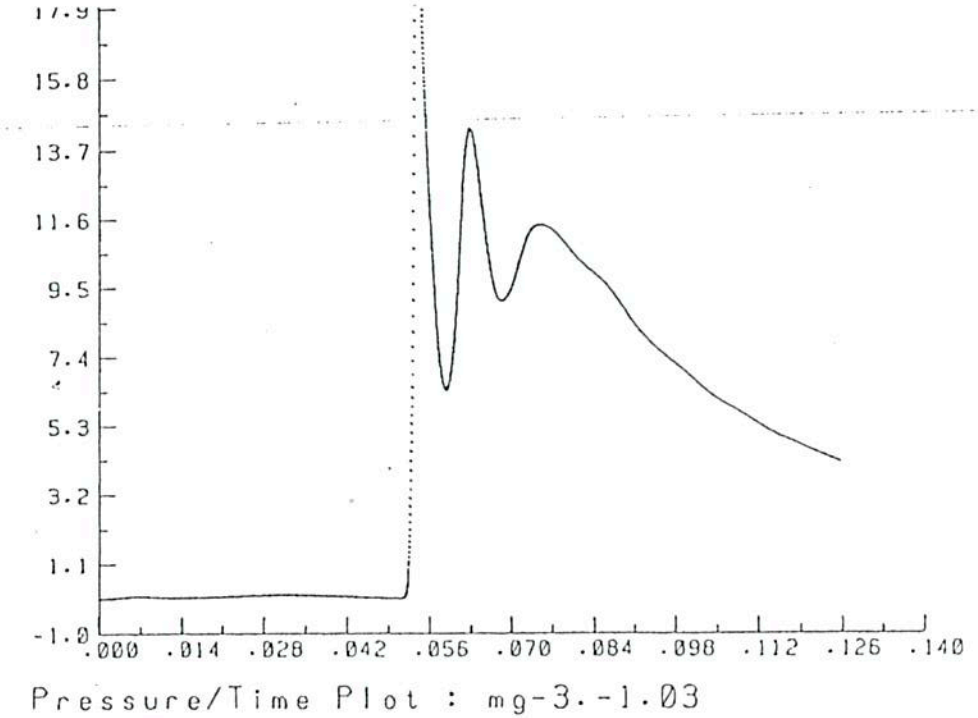

FIGURE 6.12 PRESSURE: IGNITION AT 27C/T AND NO. 4 SUPPLY ROAD

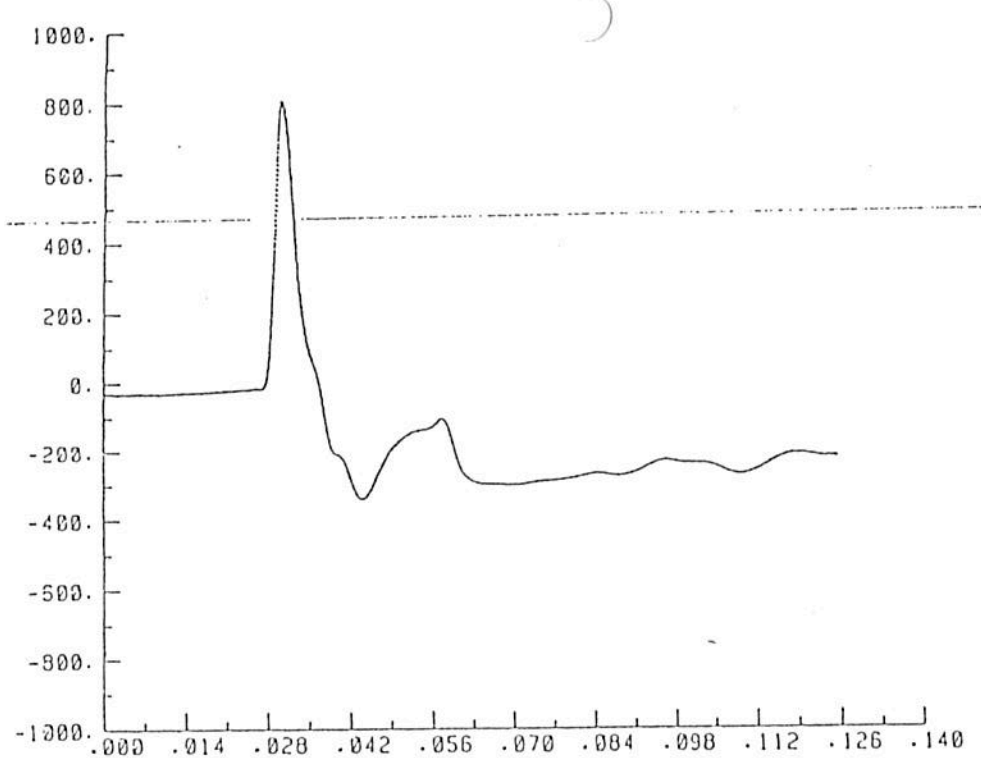

Velocity/Time Plot : mg-3.-1.10

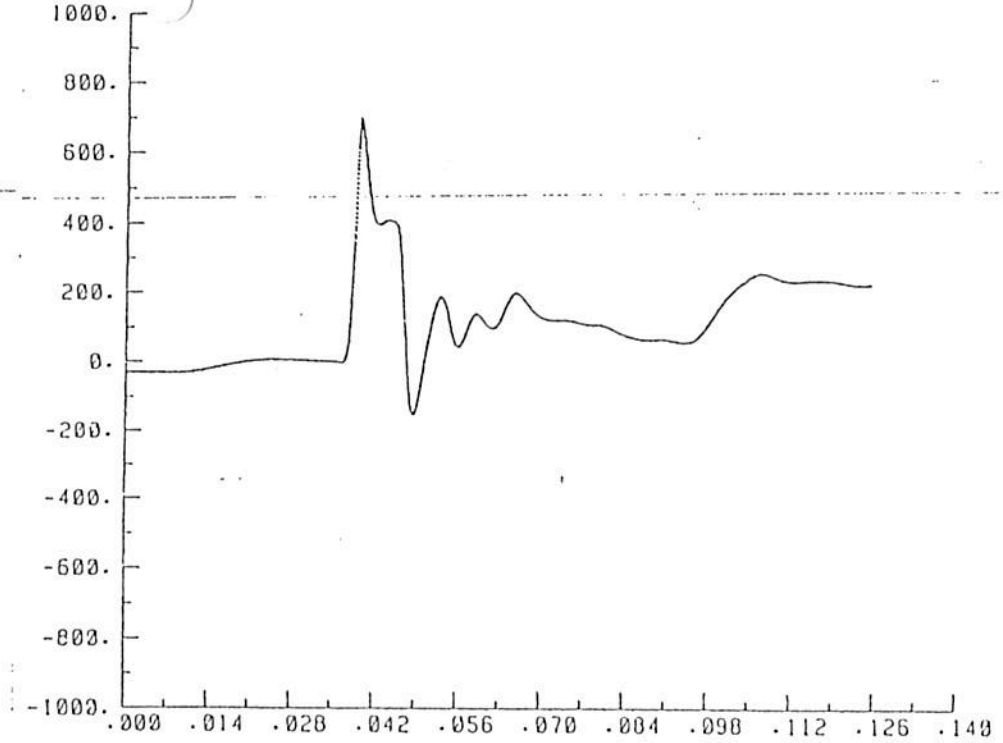

Velocity/Time Plot : mg-3.-1.07

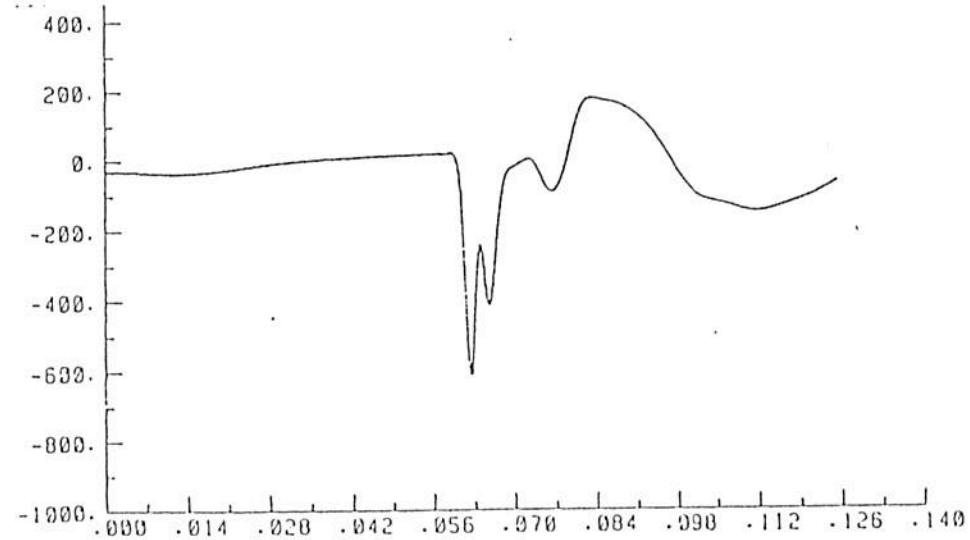

Velocity/Time Plot : mg-3.-1.02

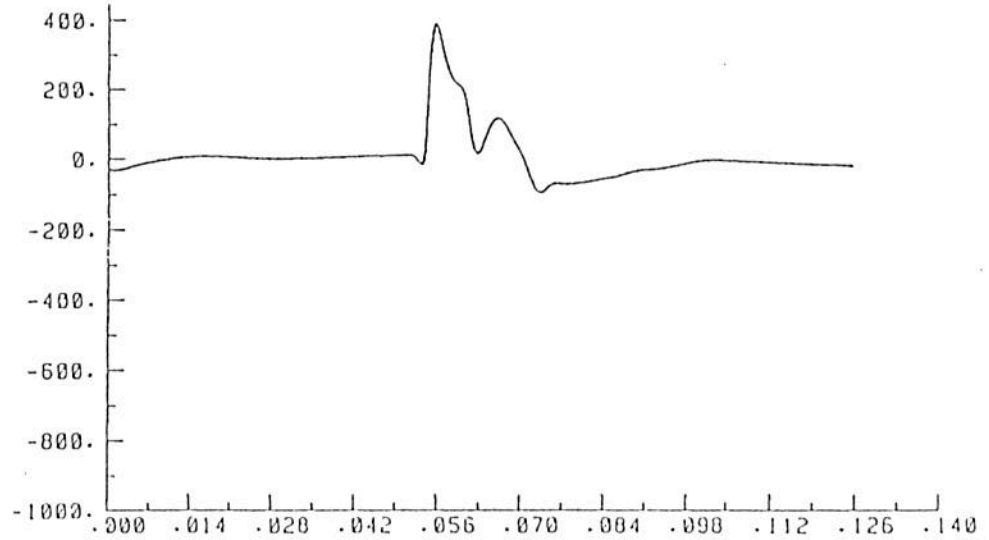

Velocity/Time Plot : mg-3.-1.03

FIGURE 6.13 U VELOCITY: IGNITION 27C/T AND NO. 4 SUPPLY ROAD

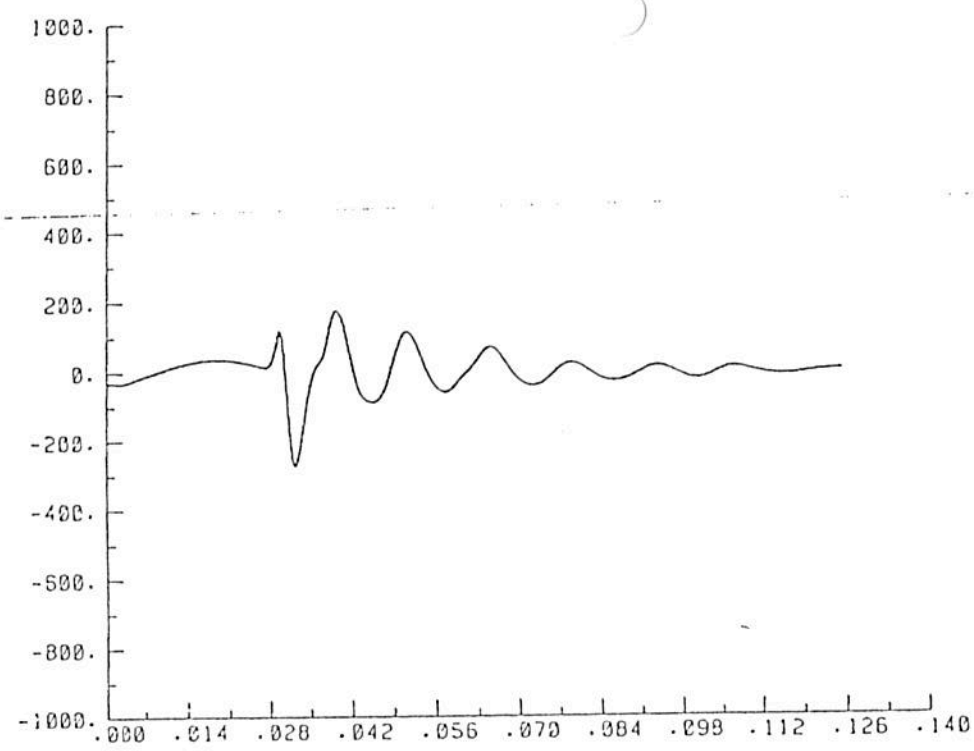

Velocity/Time Plot : mg-3.-1.10

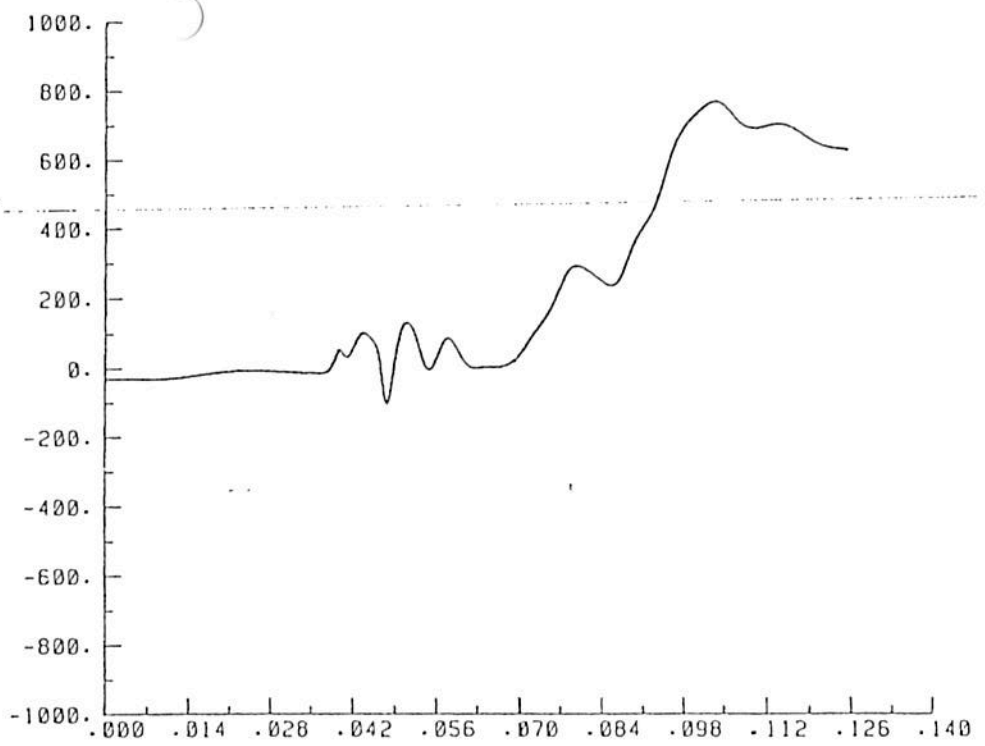

Velocity/Time Plot : mg-3.-1.07

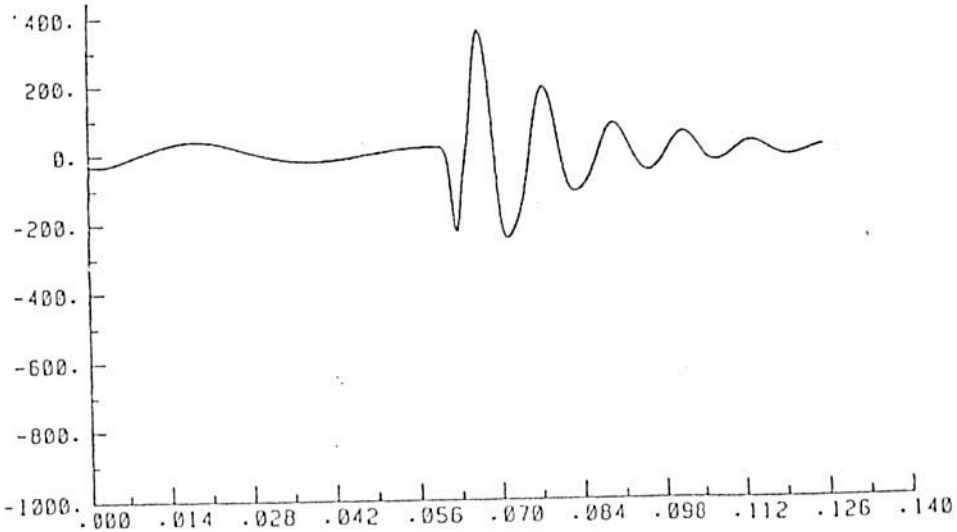

Velocity/Time Plot : mg-3.-1.02

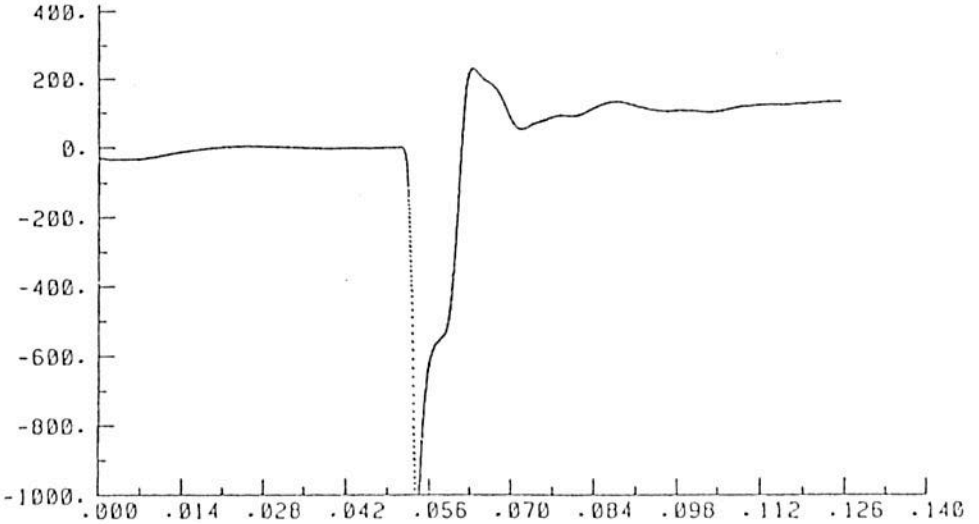

Velocity/Time Plot : mg-3.-1.03

FIGURE 6.14 V VELOCITY: IGNITION AT 27C/T AND NO. 4 SUPPLY ROAD

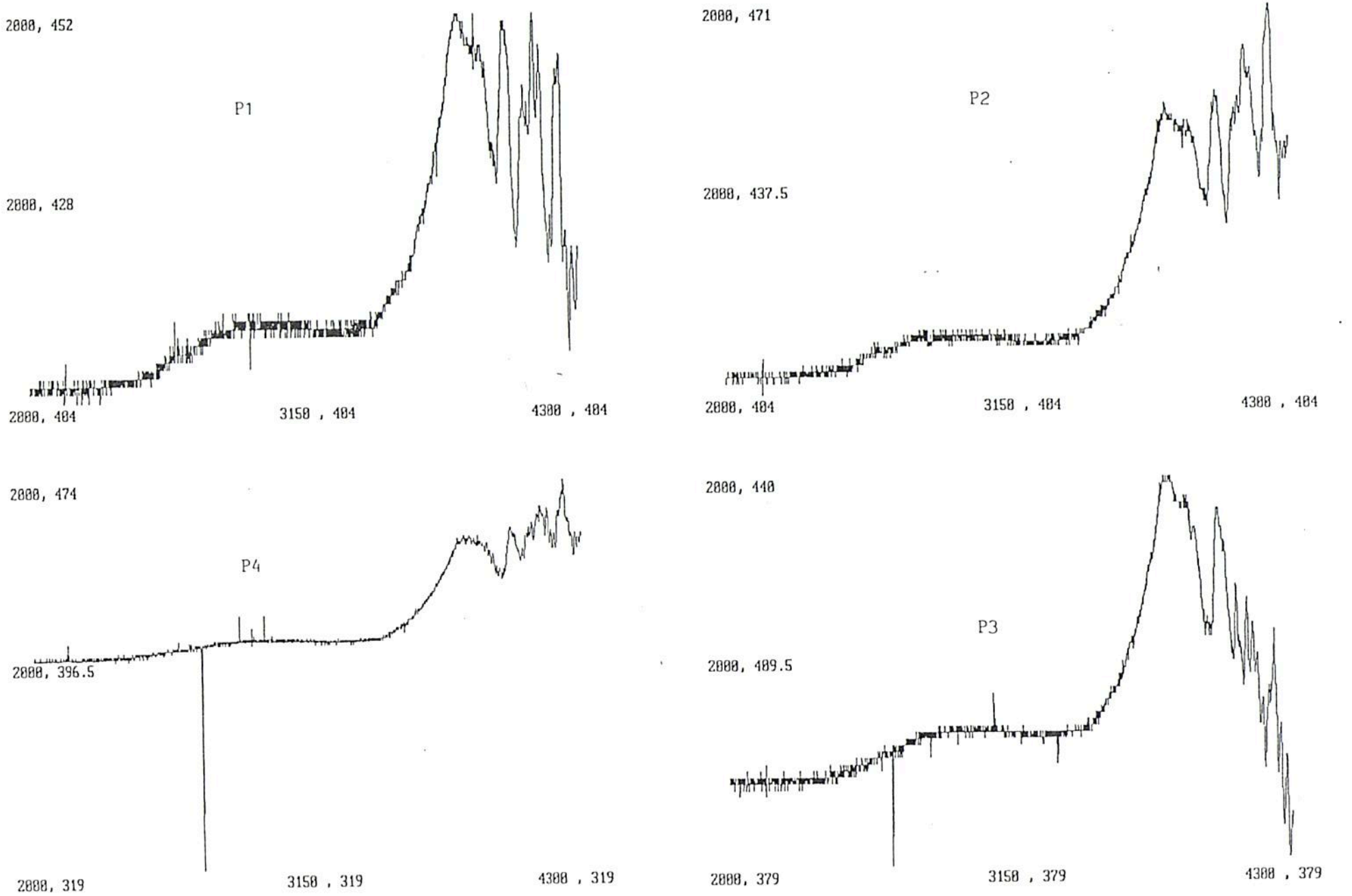

FIGURE 6.15 PRESSURE FROM SCALE MODEL EXPERIMENTS: IGNITION AT 27C/T AND NO. 4 SUPPLY ROAD

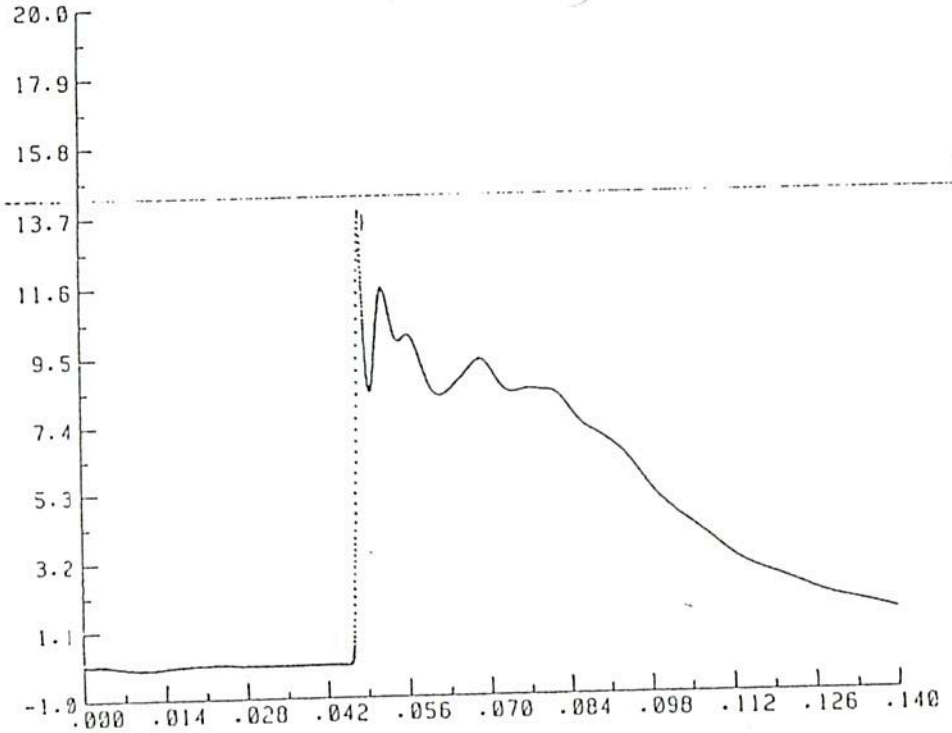

Pressure/Time Plot : mg-3.-2.10

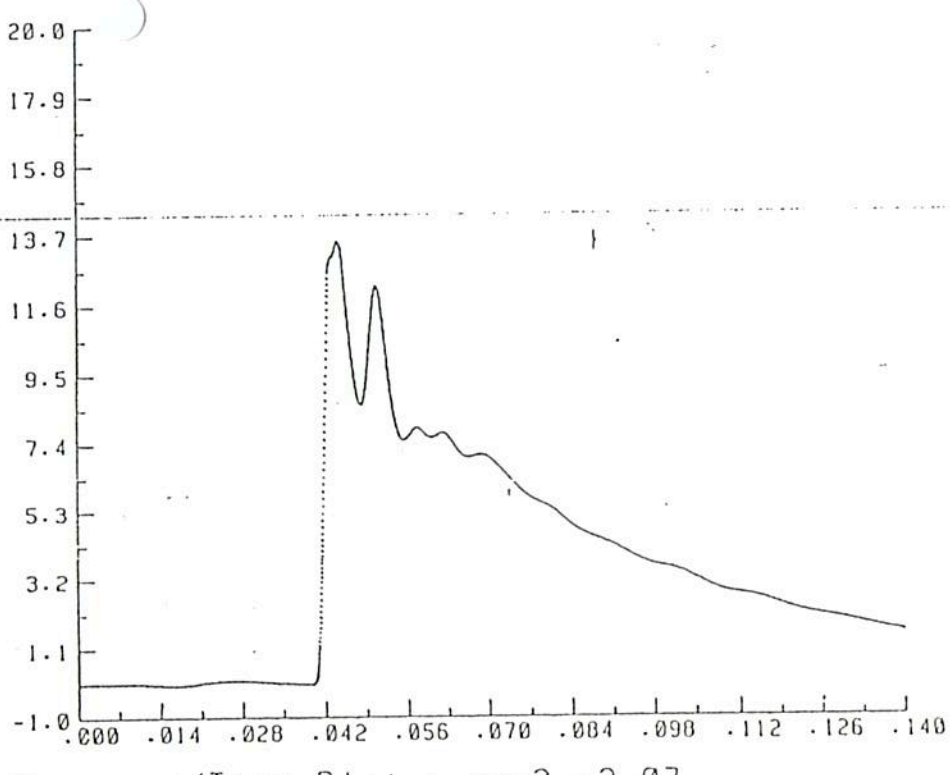

Pressure/Time Plot : mg-3.-2.07

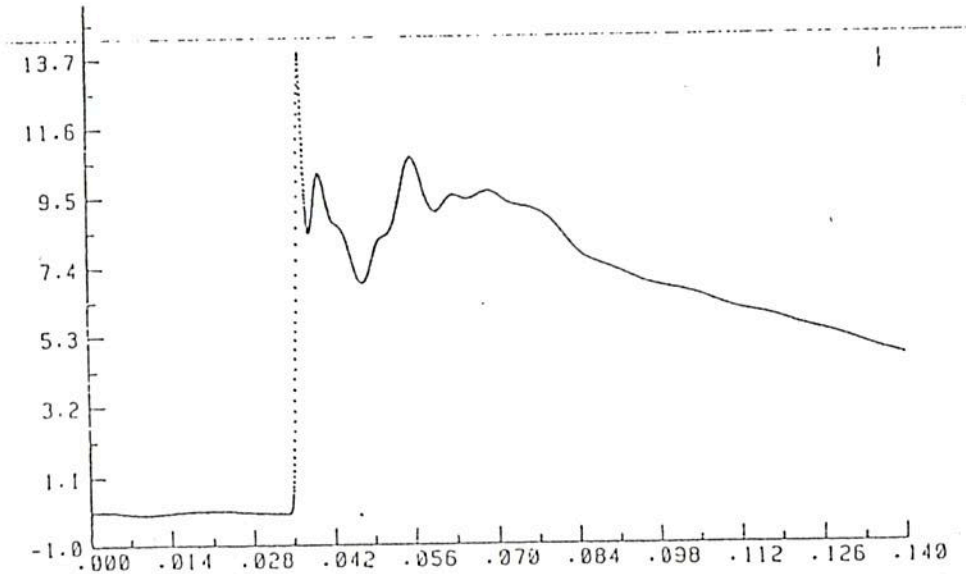

Pressure/Time Plot : mg-3.-2.02

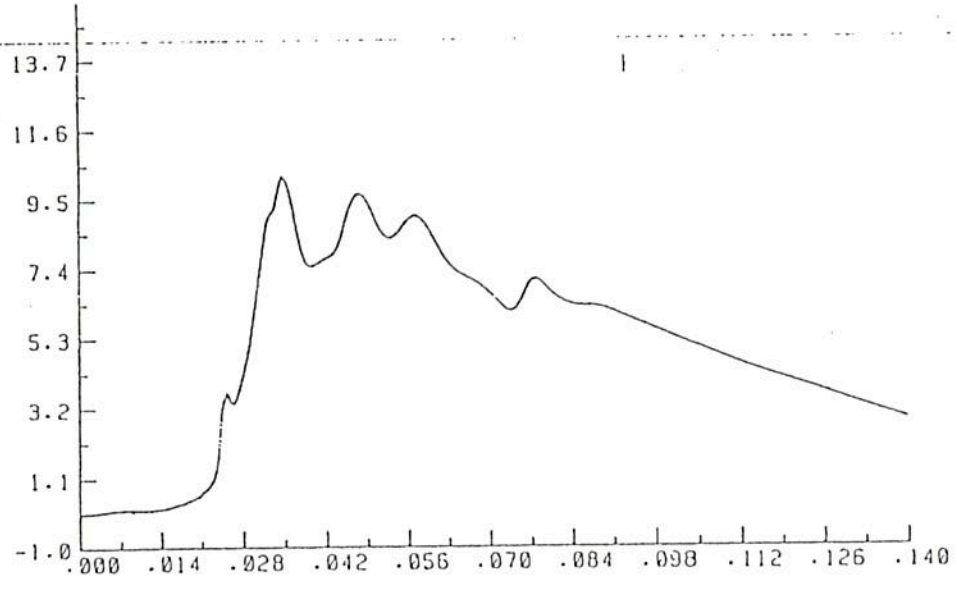

Pressure/Time Plot : mg-3.-2.03

FIG 6.16 PRESSURE IGNITION AT 26C/T & NO. 3 BELT ROAD

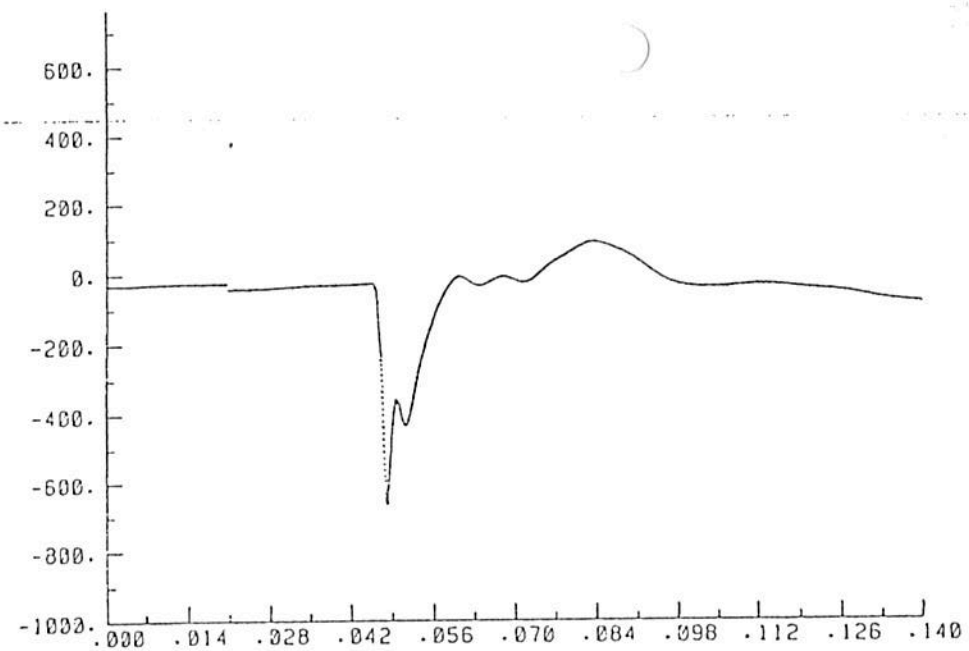

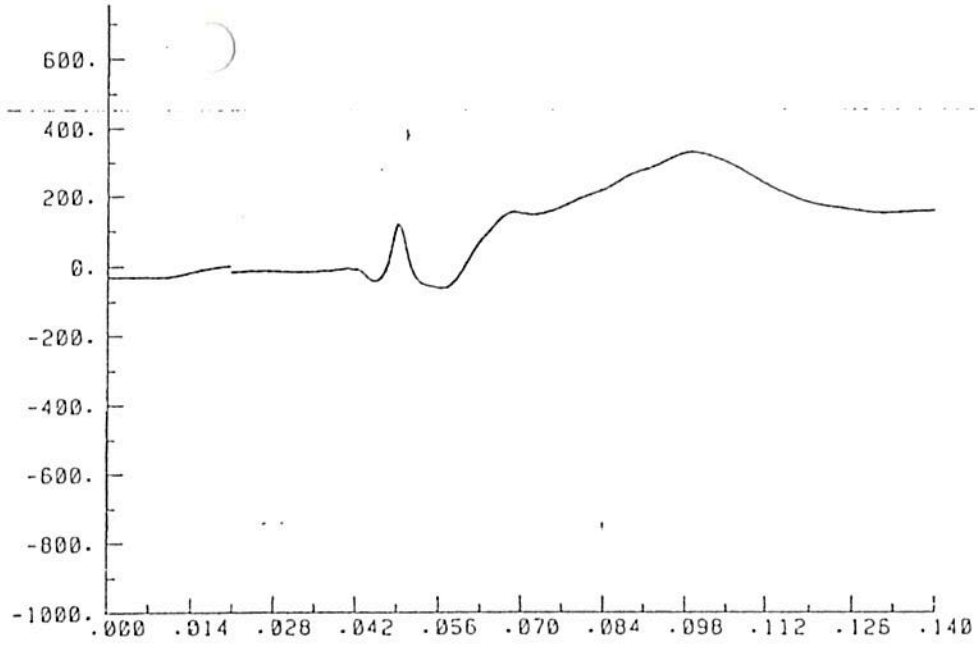

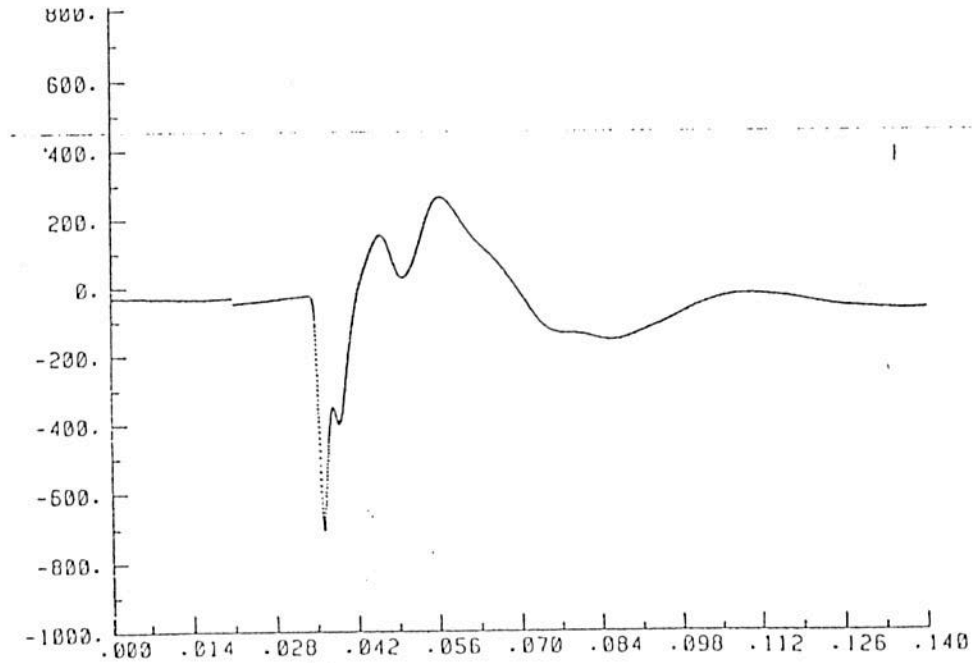

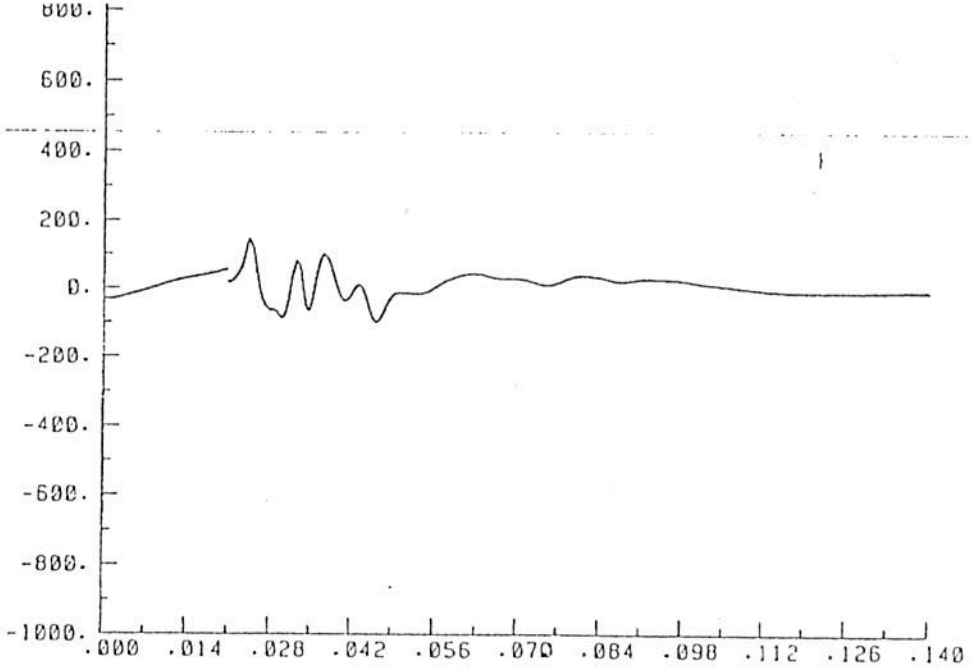

FIGURE 6.17 U VELOCITY: IGNITION AT 26C/T AND NO. 3 BELT ROAD

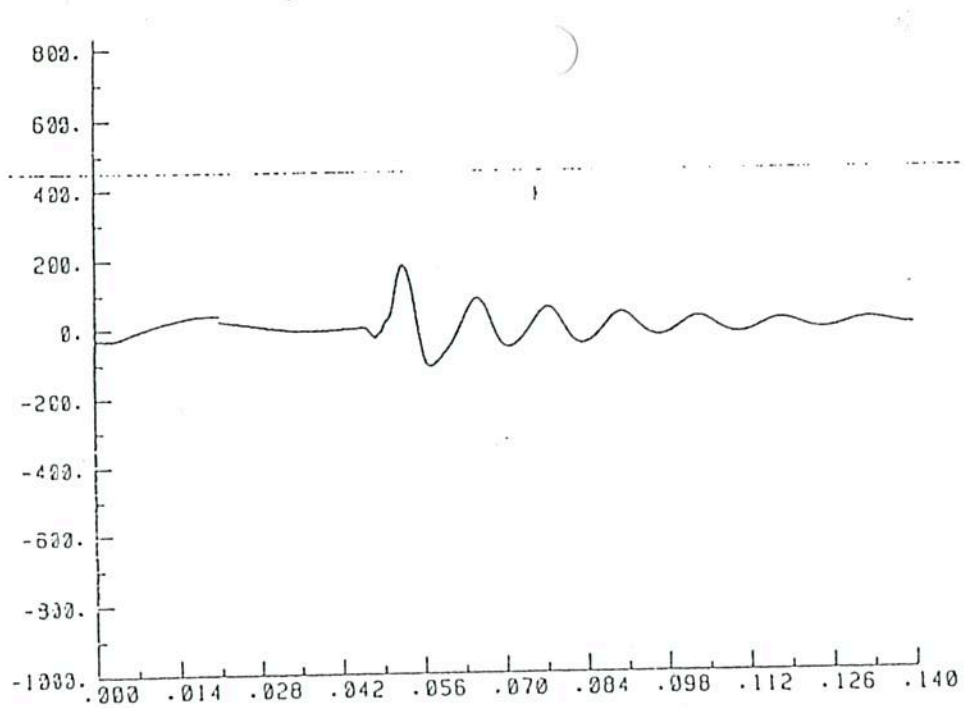

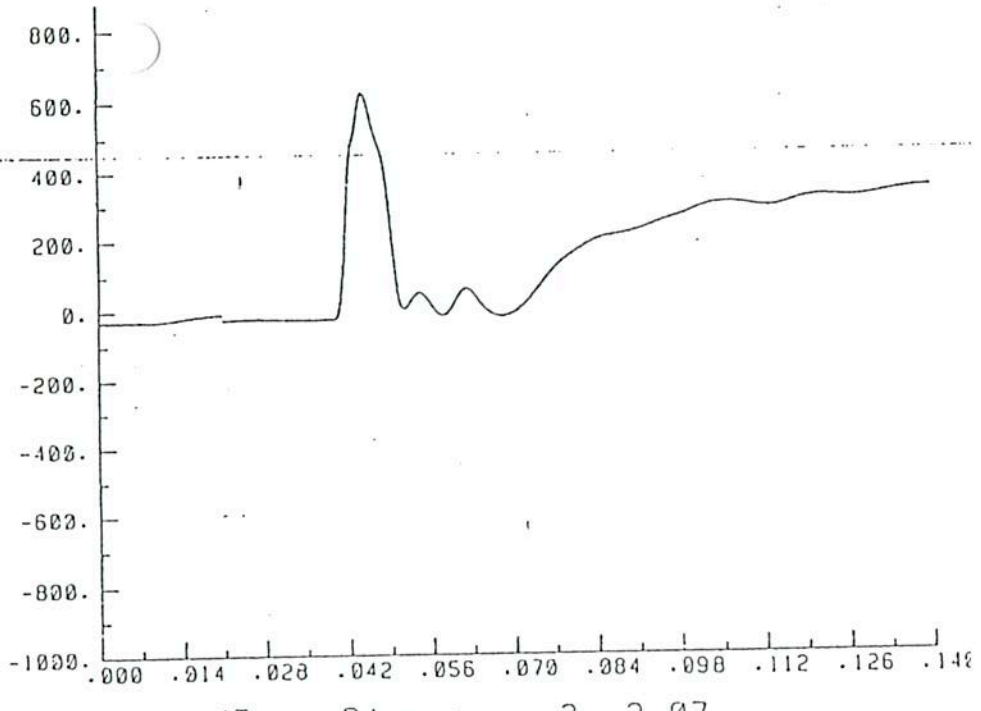

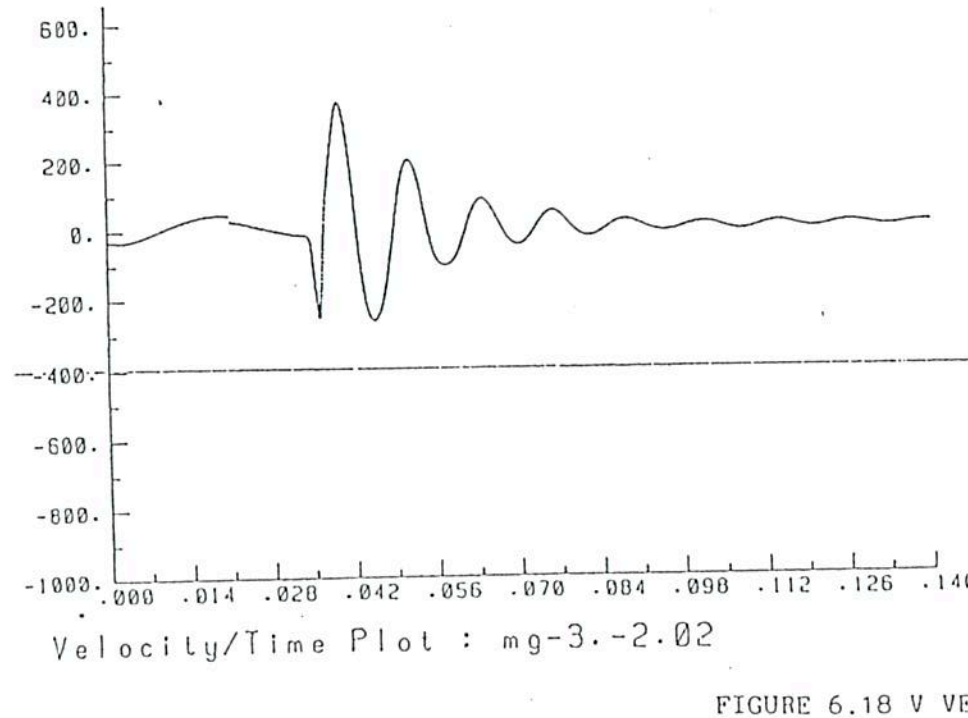

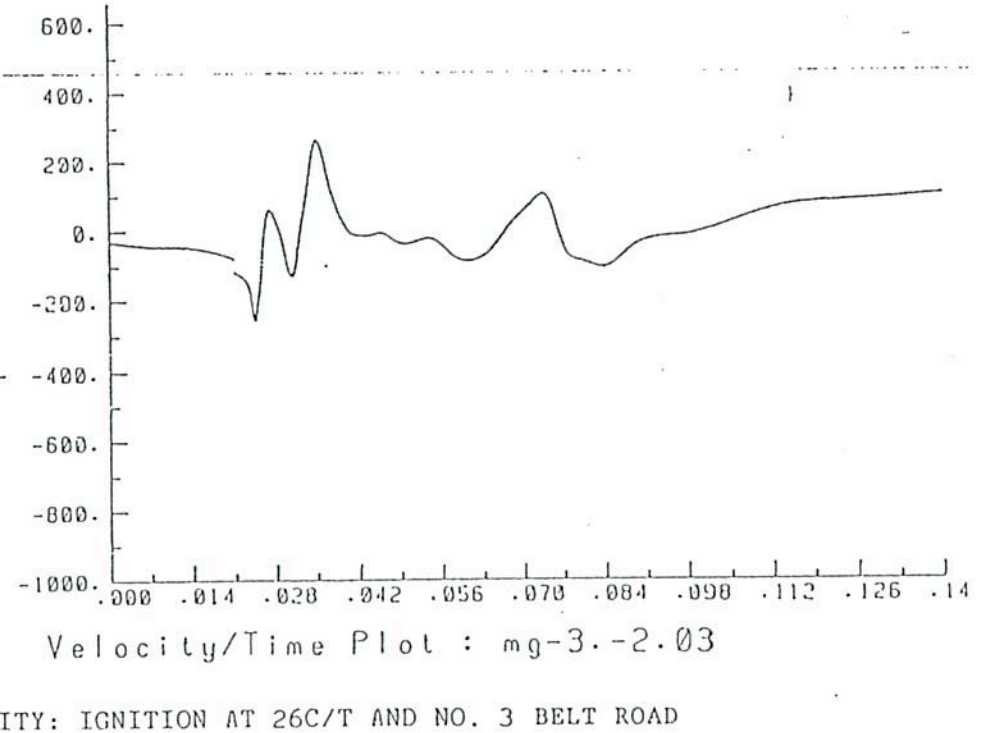

FIGURE 6.18 V VELOCITY: IGNITION AT 26C/T AND NO. 3 BELT ROAD